Analysis of an adaptive HDG method for the Brinkman problem

Rodolfo Araya, Manuel Solano, and Patrick Vega*

*CI²MA and Departamento de Ingeniería Matemática, Universidad de Concepción,
Casilla 160-C, Concepción, Chile*

rodolfo.araya@udec.cl   msolano@ing-mat.udec.cl   *Corresponding author: pvega@ing-mat.udec.cl

We introduce and analyze a hybridizable discontinuous Galerkin method for the gradient-velocity-pressure formulation of the Brinkman problem. We present an *a priori* error analysis of the method, showing optimal order of convergence of the error. We also introduce an *a posteriori* error estimator, of the residual type, which helps us to improve the quality of the numerical solution. We establish reliability and local efficiency of our estimator for the L^2-error of the velocity gradient and the pressure and the H^1-error of the velocity, with constants written explicitly in terms of the physical parameters and independent of the size of the mesh. In particular, our results are also valid for the Stokes problem. Finally, we provide numerical experiments showing the quality of our adaptive scheme.

Keywords: brinkman equations; stokes equations; hybridizable discontinuous Galerkin method; *a priori* error analysis; *a posteriori* error analysis.

1. Introduction

The main goal of this work is to introduce and analyze a hybridizable discontinuous Galerkin (HDG) method applied to the Stokes/Brinkman equations of an incompressible flow through porous media. The problem can be formulated as follows

$$L - \nabla \boldsymbol{u} = 0 \qquad \text{in } \Omega, \tag{1.1a}$$

$$- \nabla \cdot (\nu L) + \nabla p + \alpha \boldsymbol{u} = \boldsymbol{f} \qquad \text{in } \Omega, \tag{1.1b}$$

$$\nabla \cdot \boldsymbol{u} = 0 \qquad \text{in } \Omega, \tag{1.1c}$$

$$\boldsymbol{u} = \boldsymbol{u}_D \qquad \text{on } \Gamma, \tag{1.1d}$$

$$\int_{\Omega} p = 0, \tag{1.1e}$$

where $\Omega \subset \mathbb{R}^d$ ($d = 2, 3$) is a polygonal/polyhedral domain with Lipschitz boundary Γ, $\boldsymbol{u}$ is the velocity, p is the pressure, $\nu > 0$ is the effective viscosity of the fluid, $\alpha \geqslant 0$ is the quotient between the dynamic viscosity and the permeability of the media, $\boldsymbol{f} \in L^2(\Omega)^d$ is the external body force and $\boldsymbol{u}_D \in H^{1/2}(\Gamma)^d$ is the Dirichlet boundary data, assumed to satisfy $\int_\Gamma \boldsymbol{u}_D \cdot \boldsymbol{n} = 0$ for compatibility.

The Brinkman equation constitutes a generalization of the Darcy's equation $\boldsymbol{u} = -\alpha^{-1} \nabla p$ that describes the flow of a fluid through a porous mass with low particle density, i.e. a medium with high

permeability (Brinkman, 1947). It was motivated by the calculation of the viscous force exerted by a flowing fluid on a dense swarm of particles, where the model includes the viscous effect to state the equilibrium between the forces acting of a volume of fluid, i.e. the pressure gradient and the damping force, αu, caused by the porous mass. Applications of the Brinkman equation arise, for instance, from composite manufacturing (Griebel & Klitz, 2010), heat pipes (Kaya & Goldak, 2007), computational fuel cell dynamics (Li, 2005) and groundwater/oil reservoir modeling. In the last case, it is of interest to study how the fluid behaves during the transition from slow to fast flow through heterogeneous porous media with different contrasting porosities or with fractures, faults or wells. This phenomenon is described by the incompressible Navier–Stokes equation in the medium with large porosity, whereas Darcy's law could be considered in regions with small porosity. However, Darcy's equation is not enough to determine the transmission conditions across the interface between both media. That is why Brinkman equation is employed instead.

Let us briefly describe the historic perspective of the development of HDG methods. The main criticism of Discontinuous Galerkin (DG) methods is due to the fact that they have too many globally coupled degrees of freedom. In order to overcome this drawback, Cockburn *et al.* (2009b) introduced a unifying framework for hybridization of DG methods for diffusion problems, where the only globally coupled degrees of freedom are those of the numerical traces on the inter-element boundaries. The remaining unknowns are then obtained by solving local problems on each element. To be more precise, at the continuous level, the intra-element variables can be written in terms of the inter-element unknowns by solving local problems on each element. These problems, called local-solvers, can be discretized by a DG method, generating a family of methods named HDG methods. In particular, if the local solvers are approximated by the local discontinuous Galerkin (LDG) method introduced in Cockburn & Shu (1998), the resulting scheme is called LDG-hybridizable (LDG-H) as explained in Cockburn *et al.* (2009b).

In the literature, the most commonly used HDG schemes are, indeed, the LDG-H methods. Using a special projection, Cockburn *et al.* (2008) proved optimal order of convergence of a type of LDG-H method, where the stabilization parameter is set to be zero in all but one face of each element. In addition, they also provided an element-by-element postprocessing of the approximated solution having superconvergence properties. A larger class of LDG-H methods was analyzed in Cockburn *et al.* (2009a) by also using special projections. Later, Cockburn *et al.* (2010) simplified the analysis of these methods by using a technique based on a suitable designed projection inspired by the form of the numerical traces.

In addition to diffusion equations, in the context of fluid mechanics, HDG methods have been developed for a wide variety of problems such as convection–diffusion equation (Nguyen *et al.*, 2009a,b; Fu *et al.*, 2015), Stokes flow (Cockburn & Gopalakrishnan, 2009; Nguyen *et al.*, 2010; Cockburn *et al.*, 2011; Cockburn & Sayas, 2014), quasi-Newtonian Stokes flow (Gatica & Sequeira, 2015, 2016), Stokes-Darcy coupling (Gatica & Sequeira, 2017), Brinkman problem (Fu *et al.*, 2018; Gatica & Sequeira, 2018), Oseen and Navier–Stokes equations (Nguyen *et al.*, 2011; Cesmelioglu *et al.*, 2013, 2017), just to name few. Among them, we focus on those that are closely related to our work. To be more precise, Cockburn & Gopalakrishnan (2009) derived a class of HDG method for the Stokes problem considering a vorticity–velocity-pressure formulation. They showed that the method can be hybridized in four different ways including tangential velocity/pressure and velocity/average pressure hybridizations. The approach based on the velocity/average pressure hybridization was considered in Nguyen *et al.* (2010) to devise an HDG method for the velocity gradient-velocity-pressure formulation which was later analyzed by Cockburn *et al.* (2011) by employing the projection-based error analysis developed by Cockburn *et al.* (2010).

On the other hand, the first HDG method for the Brinkman problem was proposed by Fu *et al.* (2018) for a velocity gradient-velocity-pressure formulation. Recently, Gatica & Sequeira (2018) introduced and analyzed an HDG method for the Brinkman problem in pseudostress-velocity formulation.

Few contributions on the development of *a posteriori* error estimators for HDG methods can be found in the literature. Certainly, *a posteriori* error analyses of DG methods have been extensively studied. Indeed, in the context of error control in energy-like norms, we refer to Becker *et al.* (2003), Karakashian & Pascal (2003, 2007), Bustinza *et al.* (2005), Ainsworth (2007), Ern *et al.* (2007), Houston *et al.* (2007), Cochez-Dhondt & Nicaise (2008), Ern & Vohralík (2009), Lazarov *et al.* (2009), Ainsworth & Rankin (2010), Creusé & Nicaise (2010), Ern *et al.* (2010), Zhu *et al.* (2011), Creusé & Nicaise (2013), Braess *et al.* (2014), Dolejší *et al.* (2015) and Ern & Vohralík (2015). *A posteriori* error estimates to control the L^2-error of the scalar variable can be found in Rivière & Wheeler (2003) and Castillo (2005). In addition, unified frameworks of error control have been developed in Carstensen *et al.* (2009) and Lovadina & Marini (2009). A complete discussion of the aforementioned work can be found in Cockburn & Zhang (2012, 2013). The first *a posteriori* error analysis for HDG methods was carried out in Cockburn & Zhang (2012) for an LDG-H method applied to a diffusion problem. There, the authors proposed an efficient and reliable residual-based estimator that controls the error in $\boldsymbol{q}$, the gradient of the scalar variable u, which only depends on the data oscillation and on the difference between the trace of the approximation of u and its corresponding numerical trace. The construction of this estimator relies in two key ingredients. The first one is the use of an element-by-element postprocessing of the scalar variable u having superconvergence properties. The second ingredient is the Oswald interpolation operator (Karakashian & Pascal, 2003; Di Pietro & Ern, 2012) that provides a continuous approximation of a discontinuous piecewise polynomial function. Based on this technique, Cockburn & Zhang (2013) presented a unified *a posteriori* error analysis for diffusion problems. There, the authors provided an efficient and reliable error estimator for the L^2-norm of $\boldsymbol{q} - \widetilde{\boldsymbol{q}}_h$, where $\widetilde{\boldsymbol{q}}_h$ is any approximation of the flux $\boldsymbol{q}$ satisfying certain conditions (see section 2.3.1 in Cockburn & Zhang, 2013 for details). That framework allows us to obtain *a posteriori* error indicators for a wide class of method and recover well-known estimators, as well. In the context of the convection-dominated diffusion equation, Chen *et al.* (2016) proposed a reliable and locally efficient residual-based error estimator for the HDG method presented in Fu *et al.* (2015) that controls the error measured in an energy norm. This estimator is robust in the sense that the bounds of error are uniform with respect to the diffusion coefficient. The authors also employed the Oswald interpolant and considered a weighted test function technique to control the L^2-norm of the scalar solution. However, they did not use the postprocessing technique mentioned above since there is no superconvergence result for the HDG methods when the diffusion parameter is too small. An alternative approach is to use the global inf–sup condition associated to the continuous variational formulation which allows us to directly bound the error in terms of the residuals. This needs to be done carefully if applied to HDG methods since the spaces are not necessarily conforming. In this direction, Gatica & Sequeira (2016) proposed an error estimator for an augmented HDG method applied to a class of quasi-Newtonian Stokes equations in velocity gradient-pseudostress-velocity formulation. There, in order to be able to use the global inf–sup condition of the continuous problem, the numerical trace of the velocity is eliminated from the scheme by expressing it in terms of the intra-element unknowns, obtaining an equivalent discrete formulation. Moreover, the discontinuous approximation is postprocessed to construct an H(div, Ω)-conforming approximation of the pseudostress that allows us to obtain an efficient and reliable residual-based error estimator. In addition, Gatica & Sequeira (2018) employed similar techniques to propose an error estimator for an HDG method applied to the Brinkman problem in pseudostress-velocity formulation.

The main contributions of our work are the introduction of an HDG method for Brinkman equation, where the unknowns are the velocity, pressure and the gradient of the velocity, and its *a priori* and *a posteriori* analysis. Even if the Stokes case ($\alpha = 0$) has been introduced and analyzed, without an *a posteriori* analysis, in Cockburn *et al.* (2011), this is the first time that the analysis is extended for Brinkman ($\alpha \neq 0$) in the natural variables. In the *a posteriori* error analysis we propose a reliable and locally efficient residual-based *a posteriori* error estimator for both Brinkman and Stokes problems, using the Oswald interpolation operator and a postprocessing technique. As we will see in Section 2.3, we propose a *new* postprocessed approximation of the velocity suited to the Brinkman problem and show it superconverges with optimal order. In addition, all the constants in the estimates are written explicitly in terms of the physical parameters α and ν.

The paper is organized as follows. In Section 2, we introduce the HDG method, notation and basic definitions. In Section 3 we present an *a priori* error analysis for the HDG method. In Section 4, we introduce our *a posteriori* error estimator and state the main results concerning it. Finally, in Section 5 we show numerical evidence, in dimension two, that validates our theoretical result concerning the behavior of our scheme.

2. The method

2.1 *Notation*

Let $\{\mathscr{T}_h\}_{h>0}$ be a family of conforming triangulations, made of simplexes K, of the domain Ω that verifies the shape-regularity condition, i.e. there exists a positive constant σ such that $h_K/\rho_K \leqslant \sigma$ for all $K \in \mathscr{T}_h$ and for all $h > 0$, where h_K and ρ_K denote the diameter of K and the diameter of the largest ball inside K, respectively. Let h_e be the diameter of a face/edge e. From now on, we will use the word 'face' even in the context of dimension two. We denote by $\mathscr{E}_h^i$ the set of interior faces and by $\mathscr{E}_h^\partial$ the set of boundary faces. We set $\mathscr{E}_h := \mathscr{E}_h^i \cup \mathscr{E}_h^\partial$, $\partial\mathscr{T}_h := \{\partial K : K \in \mathscr{T}_h\}$, $\omega_e := \{K \in \mathscr{T}_h : e \subset \partial K\}$. We will use bold and Roman letters to denote vector- and tensor-valued variables, respectively. For a tensor-valued function G and a vector-valued function $\boldsymbol{v}$, we define

$$[\![\mathrm{G}]\!] = \begin{cases} \mathrm{G}^-\boldsymbol{n}^- + \mathrm{G}^+\boldsymbol{n}^+, & e \in \mathscr{E}_h \setminus \mathscr{E}_h^\partial \\ \boldsymbol{0}, & e \in \mathscr{E}_h^\partial \end{cases} \qquad \text{and} \qquad [\![\boldsymbol{v}]\!] = \begin{cases} \boldsymbol{v}^+ - \boldsymbol{v}^-, & e \in \mathscr{E}_h \setminus \mathscr{E}_h^\partial \\ \boldsymbol{v} - \boldsymbol{u}_D, & e \in \mathscr{E}_h^\partial, \end{cases}$$

where $\boldsymbol{n}$ denotes the outward unit normal vector to ∂K. We use the notation $(\cdot, \cdot)_D$ and $\langle \cdot, \cdot \rangle_D$ for the L^2-inner product on $D \in \mathscr{T}_h$ and $D \in \mathscr{E}_h$, respectively. Let us also define

$$\|\!|\boldsymbol{v}|\!\|_{1,D} := \left(\alpha \|\boldsymbol{v}\|_{0,D}^2 + \nu \|\nabla\boldsymbol{v}\|_{0,D}^2 \right)^{1/2}.$$

Finally, $\mathbb{P}_k(S)$ will denote the space of polynomials of total degree no greater than $k \in \mathbb{N} \cup \{0\}$, with S being a simplex or a face as appropriate.

To simplify the notation, in what follows, we will use $a \preceq b$ to denote $a \leqslant Cb$, where C is a generic constant depending only on the shape regularity constant σ, the domain Ω and the polynomial degree k, but independent of h and the physical parameters of the equation.

2.2 An HDG method for the Brinkman problem

Let us consider the following approximation spaces:

$$G_h := \{G \in L^2(\mathscr{T}_h)^{d \times d} : G|_K \in \mathbb{P}_k(K)^{d \times d} \quad \forall K \in \mathscr{T}_h\}, \tag{2.1a}$$

$$\boldsymbol{V}_h := \{\boldsymbol{v} \in L^2(\mathscr{T}_h)^d : \boldsymbol{v}|_K \in \mathbb{P}_k(K)^d \quad \forall K \in \mathscr{T}_h\}, \tag{2.1b}$$

$$P_h := \{w \in L^2(\mathscr{T}_h) : w|_T \in \mathbb{P}_k(K) \quad \forall K \in \mathscr{T}_h\}, \tag{2.1c}$$

$$\boldsymbol{M}_h := \{\boldsymbol{\mu} \in L^2(\mathscr{E}_h)^d : \boldsymbol{\mu}|_e \in \mathbb{P}_k(e)^d \quad \forall e \in \mathscr{E}_h\}. \tag{2.1d}$$

Then, based on the method developed in Nguyen *et al.* (2010) for the Stokes flow, we introduce an HDG formulation for Brinkman problem (1.1) that approximates the exact solution $(L, \boldsymbol{u}, p, \boldsymbol{u}|_{\mathscr{E}_h})$ by the only solution of the following scheme: *Find* $(L_h, \boldsymbol{u}_h, p_h, \widehat{\boldsymbol{u}}_h) \in G_h \times \boldsymbol{V}_h \times P_h \times \boldsymbol{M}_h$ *such that*

$$(L_h, G)_{\mathscr{T}_h} + (\boldsymbol{u}_h, \nabla \cdot G)_{\mathscr{T}_h} - \langle \widehat{\boldsymbol{u}}_h, G\boldsymbol{n} \rangle_{\partial \mathscr{T}_h} = 0, \tag{2.2a}$$

$$(\nu L_h, \nabla \boldsymbol{v})_{\mathscr{T}_h} - (p_h, \nabla \cdot \boldsymbol{v})_{\mathscr{T}_h} + (\alpha \boldsymbol{u}_h, \boldsymbol{v})_{\mathscr{T}_h} - \langle \nu \widehat{L}_h \boldsymbol{n} - \widehat{p}_h \boldsymbol{n}, \boldsymbol{v} \rangle_{\partial \mathscr{T}_h} = (\boldsymbol{f}, \boldsymbol{v})_{\mathscr{T}_h}, \tag{2.2b}$$

$$- (\boldsymbol{u}_h, \nabla q)_{\mathscr{T}_h} + \langle \widehat{\boldsymbol{u}}_h \cdot \boldsymbol{n}, q \rangle_{\partial \mathscr{T}_h} = 0, \tag{2.2c}$$

$$\langle \widehat{\boldsymbol{u}}_h, \boldsymbol{\mu} \rangle_\Gamma = \langle \boldsymbol{u}_D, \boldsymbol{\mu} \rangle_\Gamma, \tag{2.2d}$$

$$\langle \nu \widehat{L}_h \boldsymbol{n} - \widehat{p}_h \boldsymbol{n}, \boldsymbol{\mu} \rangle_{\partial \mathscr{T}_h \setminus \Gamma} = 0, \tag{2.2e}$$

$$(p_h, 1)_\Omega = 0, \tag{2.2f}$$

for all $(G, \boldsymbol{v}, q, \boldsymbol{\mu}) \in G_h \times \boldsymbol{V}_h \times P_h \times \boldsymbol{M}_h$. Here, $\nu \widehat{L}_h \boldsymbol{n} - \widehat{p}_h \boldsymbol{n} := \nu L_h \boldsymbol{n} - p_h \boldsymbol{n} - \nu \tau (\boldsymbol{u}_h - \widehat{\boldsymbol{u}}_h)$ on $\partial \mathscr{T}_h$ and τ is a positive stabilization function on $\partial \mathscr{T}_h$ that we assume, without loss of generality, to be of order one. For other choices of τ we refer to Cockburn *et al.* (2011).

2.3 Local postprocessing of the vector solution

One of the features of HDG method is the construction of a local element-by-element postprocessing $\boldsymbol{u}_h^*$ of $\boldsymbol{u}_h$ that approximates $\boldsymbol{u}$ with enhanced accuracy. In our case, we propose to construct $\boldsymbol{u}_h^*$ suited for the Brinkman problem as follows. We seek $\boldsymbol{u}_h^* \in \boldsymbol{V}_h^* := \{\boldsymbol{w} \in L^2(\Omega)^d : \boldsymbol{w}|_K \in \mathbb{P}_{k+1}(K)^d \ \forall K \in \mathscr{T}_h\}$ such that, for all $K \in \mathscr{T}_h$, it satisfies

$$\nu(\nabla \boldsymbol{u}_h^*, \nabla \boldsymbol{w})_K + \alpha(\boldsymbol{u}_h^*, \boldsymbol{w})_K = \nu(L_h, \nabla \boldsymbol{w})_K + \alpha(\boldsymbol{u}_h, \boldsymbol{w})_K \quad \forall \boldsymbol{w} \in \mathbb{P}_{k+1}(K)^d \tag{2.3a}$$

and, if $\alpha = 0$, also satisfies the following equation:

$$(\boldsymbol{u}_h^*, \boldsymbol{w})_K = (\boldsymbol{u}_h, \boldsymbol{w})_K \quad \forall \boldsymbol{w} \in \mathbb{P}_0(K)^d. \tag{2.3b}$$

It's straightforward to see that $\boldsymbol{u}_h^*$ is well defined. Moreover, these new approximations will play a crucial role in the *a posteriori* error analysis as we will see in Section 4.

3. *A priori* error analysis

The *a priori* error estimates are carried out by using the projection-based analysis in Cockburn *et al.* (2011), which consists of introducing a suitable projection Π_h that helps us to write the error as the sum of an approximation error and a projection of the error. To be more precise, let $(\mathrm{L}, \boldsymbol{u}, p) \in H^1(\mathscr{T}_h)^{d \times d} \times H^1(\mathscr{T}_h)^d \times H^1(\mathscr{T}_h)$. Then, $\Pi_h(\mathrm{L}, \boldsymbol{u}, p) := (\Pi_{\mathrm{G}}\mathrm{L}, \Pi_V \boldsymbol{u}, \Pi_P p) \in \mathrm{G}_h \times V_h \times P_h$ is defined as the only solution of

$$(\Pi_{\mathrm{G}}\mathrm{L}, \mathrm{G})_K = (\mathrm{L}, \mathrm{G})_K \qquad \forall\, \mathrm{G} \in \mathbb{P}_{k-1}(K)^{d \times d}, \tag{3.1a}$$

$$(\Pi_V \boldsymbol{u}, \boldsymbol{v})_K = (\boldsymbol{u}, \boldsymbol{v})_K \qquad \forall\, \boldsymbol{v} \in \mathbb{P}_{k-1}(K)^d, \tag{3.1b}$$

$$(\Pi_P p, q)_K = (p, q)_K \qquad \forall\, q \in \mathbb{P}_{k-1}(K), \tag{3.1c}$$

$$(\operatorname{tr} \Pi_{\mathrm{G}}\mathrm{L}, q)_K = (\operatorname{tr} \mathrm{L}, q)_K \qquad \forall\, q \in \mathbb{P}_k(K), \tag{3.1d}$$

$$\langle \nu \Pi_{\mathrm{G}}\mathrm{L}\boldsymbol{n} - \Pi_P p\boldsymbol{n} - \nu \Pi_V \boldsymbol{u}, \boldsymbol{\mu}\rangle_e = \langle \nu \mathrm{L}\boldsymbol{n} - p\boldsymbol{n} - \nu \boldsymbol{u}, \boldsymbol{\mu}\rangle_e \qquad \forall\, \boldsymbol{\mu} \in \mathbb{P}_k(e)^d, \tag{3.1e}$$

for all $K \in \mathscr{T}_h$ and $e \subset \partial K$. This projection has the following approximation properties.

LEMMA 3.1 Let $\ell_{\boldsymbol{u}}, \ell_\sigma, \ell_{\mathrm{L}}, \ell_p \in [0, k]$. On each $K \in \mathscr{T}_h$ it holds

$$\|\Pi_V \boldsymbol{u} - \boldsymbol{u}\|_{0,K} \preceq h_K^{\ell_{\boldsymbol{u}}+1}|\boldsymbol{u}|_{\ell_{\boldsymbol{u}}+1,K} + h_K^{\ell_\sigma+1}\nu^{-1}|\nabla \cdot (\nu\mathrm{L} - p\mathrm{I})|_{\ell_\sigma,K},$$

$$\|\Pi_{\mathrm{G}}\mathrm{L} - \mathrm{L}\|_{0,K} \preceq h_K^{\ell_{\mathrm{L}}+1}|\mathrm{L}|_{\ell_{\mathrm{L}}+1,K} + \|\Pi_V \boldsymbol{u} - \boldsymbol{u}\|_{0,K} + h_K^{\ell_{\boldsymbol{u}}+1}|\boldsymbol{u}|_{\ell_{\boldsymbol{u}}+1,K},$$

$$\|\Pi_P p - p\|_{0,K} \preceq h_K^{\ell_p+1}|p|_{\ell_p+1,K} + \nu\|\Pi_{\mathrm{G}}\mathrm{L} - \mathrm{L}\|_{0,K} + h_K^{\ell_{\mathrm{L}}+1}\nu|\mathrm{L}|_{\ell_{\mathrm{L}}+1,K}.$$

Proof. See Theorems 2.1 and 2.3 in Cockburn *et al.* (2011). $\qquad\qquad\square$

Now, let $\mathsf{P}_M \boldsymbol{u}$ be the L^2-projection of $\boldsymbol{u}$ into $\boldsymbol{M}_h$. Then, the projection of the errors $\Pi_{\mathrm{G}}\mathrm{L} - \mathrm{L}_h$, $\Pi_V \boldsymbol{u} - \boldsymbol{u}_h$, $\mathsf{P}_M \boldsymbol{u} - \widehat{\boldsymbol{u}}_h$ and $\Pi_P p - p_h$ satisfies the following equations.

LEMMA 3.2 For all $(\mathrm{G}, \boldsymbol{v}, q, \boldsymbol{\mu}) \in \mathrm{G}_h \times V_h \times P_h \times \boldsymbol{M}_h$ it holds

$$(\Pi_{\mathrm{G}}\mathrm{L} - \mathrm{L}_h, \mathrm{G})_{\mathscr{T}_h} + (\Pi_V \boldsymbol{u} - \boldsymbol{u}_h, \nabla \cdot \mathrm{G})_{\mathscr{T}_h} - \langle \mathsf{P}_M \boldsymbol{u} - \widehat{\boldsymbol{u}}_h, \mathrm{G}\boldsymbol{n}\rangle_{\partial \mathscr{T}_h} = (\Pi_{\mathrm{G}}\mathrm{L} - \mathrm{L}, \mathrm{G})_{\mathscr{T}_h},$$

$$-(\nabla \cdot (\nu(\Pi_{\mathrm{G}}\mathrm{L} - \mathrm{L}_h)), \boldsymbol{v})_{\mathscr{T}_h} + \alpha(\Pi_V \boldsymbol{u} - \boldsymbol{u}_h, \boldsymbol{v})_{\mathscr{T}_h} + (\nabla(\Pi_P p - p_h), \boldsymbol{v})_{\mathscr{T}_h}$$
$$+\nu\langle \Pi_V \boldsymbol{u} - \boldsymbol{u}_h - \mathsf{P}_M \boldsymbol{u} + \widehat{\boldsymbol{u}}_h, \boldsymbol{v}\rangle_{\partial \mathscr{T}_h} = 0,$$

$$-(\Pi_V \boldsymbol{u} - \boldsymbol{u}_h, \nabla q)_{\mathscr{T}_h} + \langle \mathsf{P}_M \boldsymbol{u} - \widehat{\boldsymbol{u}}_h, q\boldsymbol{n}\rangle_{\partial \mathscr{T}_h} = 0,$$

$$\langle \mathsf{P}_M \boldsymbol{u} - \widehat{\boldsymbol{u}}_h, \boldsymbol{\mu}\rangle_\Gamma = 0,$$

$$\langle \nu(\Pi_{\mathrm{G}}\mathrm{L} - \mathrm{L}_h)\boldsymbol{n} - (\Pi_P p - p_h)\boldsymbol{n} - (\Pi_V \boldsymbol{u} - \boldsymbol{u}_h - \mathsf{P}_M \boldsymbol{u} + \widehat{\boldsymbol{u}}_h), \boldsymbol{\mu}\rangle_{\partial \mathscr{T}_h \setminus \Gamma} = 0,$$

$$(\Pi_P p - p_h, 1)_\Omega = (\Pi_P p - p, 1)_\Omega.$$

Proof. The result is an extension of Lemma 3.1 in Cockburn *et al.* (2011) to our HDG method. $\qquad\square$

LEMMA 3.3 We have

$$\nu\|\Pi_{\mathrm{G}}\mathrm{L} - \mathrm{L}_h\|_{0,\mathscr{T}_h}^2 + \alpha\|\Pi_V \boldsymbol{u} - \boldsymbol{u}_h\|_{0,\mathscr{T}_h}^2 + \nu\|\Pi_V \boldsymbol{u} - \boldsymbol{u}_h - (\mathsf{P}_M \boldsymbol{u} - \widehat{\boldsymbol{u}}_h)\|_{0,\partial \mathscr{T}_h}^2 = \nu(\Pi_{\mathrm{G}}\mathrm{L} - \mathrm{L}, \Pi_{\mathrm{G}}\mathrm{L} - \mathrm{L}_h)_{\mathscr{T}_h}.$$

Proof. It follows by taking $G = \nu(\Pi_G L - L_h)$, $\boldsymbol{v} = \Pi_V \boldsymbol{u} - \boldsymbol{u}_h$, $q = \Pi_P p - p_h$ and $\boldsymbol{\mu} = P_M \boldsymbol{u} - \widehat{\boldsymbol{u}}_h$ in the first five equations of Lemma 3.2 and adding them up. $\qquad\square$

Let us emphasize that, if $\alpha \neq 0$, Lemma 3.3 provides a bound for all the projection of the errors in terms of the approximation error $\|\Pi_G L - L_h\|_{0,\mathscr{T}_h}$. As a consequence, if the solution is smooth enough, this lemma guarantees that the L^2-norm of the error of all the variables is of order h^{k+1}. On the other hand, by a duality argument, it is possible to show that actually $\|\Pi_V \boldsymbol{u} - \boldsymbol{u}_h\|_{0,\mathscr{T}_h}$ is of order h^{k+2} under regularity assumptions. More precisely, given $\boldsymbol{\theta} \in L^2(\Omega)^d$, let $(\Phi, \boldsymbol{\phi}, \phi)$ be the solution of

$$\Phi + \nabla\boldsymbol{\phi} = 0 \quad \text{in } \Omega, \tag{3.2a}$$

$$\nabla \cdot (\nu\Phi) - \nabla\phi + \alpha\boldsymbol{\phi} = \boldsymbol{\theta} \quad \text{in } \Omega, \tag{3.2b}$$

$$-\nabla \cdot \boldsymbol{\phi} = 0 \quad \text{in } \Omega, \tag{3.2c}$$

$$\boldsymbol{\phi} = \boldsymbol{0} \quad \text{on } \partial\Omega. \tag{3.2d}$$

Since $\boldsymbol{\theta} - \alpha\boldsymbol{\phi} \in L^2(\Omega)^d$, (3.2) has the same regularity as the Stokes problem. Hence, we assume $\Phi \in H^1(\Omega)^{d\times d}$, $\boldsymbol{\phi} \in H^2(\Omega)^d$ and $\phi \in H^1(\Omega)$. This assumption holds, for instance, if Ω is convex (Kellogg & Osborn, 1976; Dauge, 1989). In addition, we assume

$$\nu\|\Phi\|_{1,\Omega} + \alpha\|\boldsymbol{\phi}\|_{2,\Omega} + \|\phi\|_{1,\Omega} \preceq \|\boldsymbol{\theta}\|_{0,\Omega}. \tag{3.3}$$

LEMMA 3.4 If the elliptic regularity estimate (3.3) holds, we have

$$\|\Pi_V \boldsymbol{u} - \boldsymbol{u}_h\|_{0,\mathscr{T}_h} \preceq \left(h^{\min\{k,1\}} + \alpha^{1/2}h\right) \|\Pi_G L - L\|_{0,\mathscr{T}_h}.$$

Proof. We follow the ideas on Cockburn *et al.* (2011). Let $\boldsymbol{\theta} \in L^2(\Omega)^d$. Using (3.1), (3.2) and Lemma 3.2, we obtain

$$(\Pi_V \boldsymbol{u} - \boldsymbol{u}_h, \boldsymbol{\theta})_{\mathscr{T}_h} = \nu(\Pi_G L - L, \Phi - P_{k-1}\Phi)_{\mathscr{T}_h} + \nu(L_h - L, \Pi_G\Phi - \Phi)_{\mathscr{T}_h} + \alpha(\Pi_V \boldsymbol{u} - \boldsymbol{u}_h, \boldsymbol{\phi} - \Pi_V\boldsymbol{\phi})_{\mathscr{T}_h},$$

where $P_k \boldsymbol{u}$ is the L^2-projection of $\boldsymbol{u}$ into $\mathbb{P}_k(K)^d$.

We notice that $\nu\|\Phi - P_{k-1}\Phi\|_{0,\mathscr{T}_h} \preceq \nu h^{\min\{k,1\}}\|\Phi\|_{\min\{k,1\},\Omega} \preceq h^{\min\{k,1\}}\|\boldsymbol{\theta}\|_{0,\Omega}$. Moreover, applying the first two estimates of Lemma 3.1 to the solution of (3.2) (with $\ell_\sigma = 0$ and $\ell_{\boldsymbol{u}} = \min\{k,1\}$) and (3.3), we have that $\nu\|\Phi - \Pi_G\Phi\|_{0,K} \preceq h_K^{\min\{k,1\}}\|\boldsymbol{\theta}\|_{0,K}$. From Lemma 3.3 we get $\alpha^{1/2}\|\Pi_V \boldsymbol{u} - \boldsymbol{u}_h\|_{0,\mathscr{T}_h} \leqslant \nu^{1/2}\|\Pi_G L - L\|_{0,\mathscr{T}_h}$ and, thanks to the first estimate of Lemma 3.1 applied to $\boldsymbol{\phi}$ and by (3.3), we obtain that $\alpha^{1/2}\|\boldsymbol{\phi} - \Pi_V\boldsymbol{\phi}\|_{0,\mathscr{T}_h} \preceq \alpha^{1/2}h\|\boldsymbol{\theta}\|_{0,\Omega}$. The result follows by applying Cauchy–Schwarz inequality to the above identity and taking $\boldsymbol{\theta} = \Pi_V \boldsymbol{u} - \boldsymbol{u}_h$. $\qquad\square$

LEMMA 3.5 We have $\|\Pi_P p - p_h - \overline{\Pi_P p - p_h}\|_{0,\mathscr{T}_h} \preceq \nu\|\Pi_G L - L\|_{0,\mathscr{T}_h}$, where $\overline{q}$ is the average of q over Ω.

Proof. The result follows using Lemma 3.2 and proceeding as in Propositions 3.4 and 3.9 in Cockburn *et al.* (2011). $\qquad\square$

In the next results, we summarize the *a priori* error estimates of our numerical scheme.

THEOREM 3.6 Let $(L, \boldsymbol{u}, p)$ and $(L_h, \boldsymbol{u}_h, p_h, \widehat{\boldsymbol{u}}_h)$ be the solution of (1.1) and (2.2), respectively. Then

$$\|L - L_h\|_{0,\mathscr{T}_h} \preceq \|\Pi_G L - L_h\|_{0,\mathscr{T}_h}, \tag{3.4a}$$

$$\|p - p_h\|_{0,\mathscr{T}_h} \preceq \|\Pi_P p - p\|_{0,\mathscr{T}_h} + \nu \|\Pi_G L - L\|_{0,\mathscr{T}_h}, \tag{3.4b}$$

$$\alpha^{1/2}\|\boldsymbol{u} - \boldsymbol{u}_h\|_{0,\mathscr{T}_h} \preceq \nu^{1/2}\|\Pi_G L - L_h\|_{0,\mathscr{T}_h} + \alpha^{1/2}\|\Pi_V \boldsymbol{u} - \boldsymbol{u}\|_{0,\mathscr{T}_h}. \tag{3.4c}$$

Moreover, if (3.3) holds, then

$$\|\boldsymbol{u} - \boldsymbol{u}_h\|_{0,\mathscr{T}_h} \leqslant \|\Pi_V \boldsymbol{u} - \boldsymbol{u}\|_{0,\mathscr{T}_h} + \left(h^{\min\{k,1\}} + (\alpha/\nu)^{1/2}h\right)\|\Pi_G L - L\|_{0,\mathscr{T}_h}. \tag{3.4d}$$

Proof. It is consequence of Lemmas 3.4, 3.5 and equation (3.3), considering that $\|\overline{\Pi_P p - p_h}\|_{0,\mathscr{T}_h} \leqslant \|\Pi_P p - p_h\|_{0,\Omega}$. □

THEOREM 3.7 Let $\boldsymbol{u}_h^*$ be the approximation defined in (2.3) and assume that (3.3) holds, then

$$\|\boldsymbol{u} - \boldsymbol{u}_h^*\|_{0,\mathscr{T}_h} \preceq \left(1 + (\alpha/\nu)^{1/2}h\right)h^{l_{\boldsymbol{u}}+2}|\boldsymbol{u}|_{l_{\boldsymbol{u}}+2,\mathscr{T}_h} + \|\Pi_V \boldsymbol{u} - \boldsymbol{u}_h\|_{0,\mathscr{T}_h} + h\|L - L_h\|_{0,\mathscr{T}_h}$$
$$+ (\alpha/\nu)^{1/2}h(\|\boldsymbol{u} - \boldsymbol{u}_h\|_{0,\mathscr{T}_h} + \|\Pi_V \boldsymbol{u} - \boldsymbol{u}_h\|_{0,\mathscr{T}_h}), \tag{3.5a}$$

$$\nu^{1/2}|\boldsymbol{u} - \boldsymbol{u}_h^*|_{1,\mathscr{T}_h} \preceq (\nu^{1/2} + \alpha^{1/2}h)h^{l_{\boldsymbol{u}}+1}|\boldsymbol{u}|_{l_{\boldsymbol{u}}+2,\mathscr{T}_h} + \nu^{1/2}\|L - L_h\|_{0,\mathscr{T}_h}$$
$$+ \alpha^{1/2}(\|\boldsymbol{u} - \boldsymbol{u}_h\|_{0,\mathscr{T}_h} + \|\Pi_V \boldsymbol{u} - \boldsymbol{u}_h\|_{0,\mathscr{T}_h}), \tag{3.5b}$$

$$\sum_{e \in \mathscr{E}_h} h_e^{1/2}\|[\![\boldsymbol{u}_h^*]\!]\|_{0,e} \preceq \|\boldsymbol{u} - \boldsymbol{u}_h^*\|_{0,\mathscr{T}_h}^{1/2}\left(\|\boldsymbol{u} - \boldsymbol{u}_h^*\|_{0,\mathscr{T}_h}^2 + h^2|\boldsymbol{u} - \boldsymbol{u}_h^*|_{1,\mathscr{T}_h}^2\right)^{1/4}. \tag{3.5c}$$

Proof. Let $\mathsf{P}_{V^*}\boldsymbol{u}$ be the L^2-projection of $\boldsymbol{u}$ into V_h^* and decompose

$$\boldsymbol{u} - \boldsymbol{u}_h^* = (\boldsymbol{u} - \mathsf{P}_{V^*}\boldsymbol{u}) + \boldsymbol{w} + \mathsf{P}_0(\mathsf{P}_{V^*}\boldsymbol{u} - \boldsymbol{u}_h^*), \tag{3.6}$$

where $\boldsymbol{w} := (\mathsf{I} - \mathsf{P}_0)(\mathsf{P}_{V^*}\boldsymbol{u} - \boldsymbol{u}_h^*)$ and $P_0 \boldsymbol{v}$ is the L^2-projection of $\boldsymbol{v}$ into $\mathbb{P}_0(K)^d$. Let us first point out two key ingredients in this proof. We observe that the definition of $\boldsymbol{u}_h^*$ implies

$$\mathsf{P}_0 \boldsymbol{u}_h = \mathsf{P}_0 \boldsymbol{u}_h^*. \tag{3.7}$$

This is clearly true if $\alpha = 0$ because of (2.3b). If $\alpha \neq 0$, this identity is obtained by taking $\boldsymbol{w} = (1, 0)$ and $\boldsymbol{w} = (0, 1)$ in (2.3a). In addition, for each $K \in \mathscr{T}_h$ we notice that

$$\|\mathsf{P}_0(\mathsf{P}_{V^*}\boldsymbol{u} - \boldsymbol{u}_h)\|_{0,K} = \|\mathsf{P}_0(\Pi_V \boldsymbol{u} - \boldsymbol{u}_h)\|_{0,K} \leqslant \|\Pi_V \boldsymbol{u} - \boldsymbol{u}_h\|_{0,K}. \tag{3.8}$$

Now, let $K \in \mathscr{T}_h$. We recall the approximation property of the L^2-projection P_{V^*}:

$$\|\boldsymbol{u} - \mathsf{P}_{V^*}\boldsymbol{u}\|_{0,K} \preceq h_K^{l_{\boldsymbol{u}}+2}|\boldsymbol{u}|_{l_{\boldsymbol{u}}+2,K}. \tag{3.9}$$

Then, combining (3.6)–(3.9) and the fact that $\|\boldsymbol{w}\|_{0,K} \preceq h_K |\boldsymbol{w}|_{1,K}$ (Payne & Weinberger, 1960), we get

$$\|\boldsymbol{u} - \boldsymbol{u}_h^*\|_{0,K} \preceq h_K^{l_{\boldsymbol{u}}+2}|\boldsymbol{u}|_{l_{\boldsymbol{u}}+2,K} + \|\Pi_V \boldsymbol{u} - \boldsymbol{u}_h\|_{0,K} + h_K|\boldsymbol{w}|_{1,K}. \tag{3.10a}$$

Moreover,

$$\nu^{1/2}|\boldsymbol{u} - \boldsymbol{u}_h^*|_{1,K} \preceq \nu^{1/2}h_K^{l_{\boldsymbol{u}}+1}|\boldsymbol{u}|_{l_{\boldsymbol{u}}+2,K} + \nu^{1/2}|\boldsymbol{w}|_{1,K}. \tag{3.10b}$$

On the other hand, adding and subtracting $\alpha(\boldsymbol{u}, \boldsymbol{w})_K$ to the right-hand side of (2.3a) and considering that $\mathrm{L} = \nabla \boldsymbol{u}$, we obtain

$$\nu(\nabla \boldsymbol{u}_h^*, \nabla \boldsymbol{w})_K + \alpha(\boldsymbol{u}_h^*, \boldsymbol{w})_K = \nu(\mathrm{L}_h - \mathrm{L}, \nabla \boldsymbol{w})_K + \alpha(\boldsymbol{u}_h - \boldsymbol{u}, \boldsymbol{w})_K + \nu(\nabla \boldsymbol{u}, \nabla \boldsymbol{w})_K + \alpha(\boldsymbol{u}, \boldsymbol{w})_K.$$

This identity, together with (3.7), implies

$$\nu|\boldsymbol{w}|_{1,K}^2 + \alpha\|\boldsymbol{w}\|_{0,K}^2 = \nu(\mathrm{L} - \mathrm{L}_h, \nabla \boldsymbol{w})_K + \alpha(\boldsymbol{u} - \boldsymbol{u}_h, \boldsymbol{w})_K + \nu(\nabla(\mathsf{P}_{V^*}\boldsymbol{u} - \boldsymbol{u}), \nabla \boldsymbol{w})_K + \alpha(\mathsf{P}_{V^*}\boldsymbol{u} - \boldsymbol{u}, \boldsymbol{w})_K$$
$$- \alpha(\mathsf{P}_0(\mathsf{P}_{V^*}\boldsymbol{u} - \boldsymbol{u}_h), \boldsymbol{w})_K.$$

Then, thanks to Cauchy–Schwarz inequality, (3.8) and the approximation property (3.9), we get

$$\nu^{1/2}|\boldsymbol{w}|_{1,K} + \alpha^{1/2}\|\boldsymbol{w}\|_{0,K} \preceq \nu^{1/2}\|\mathrm{L} - \mathrm{L}_h\|_{0,K} + \alpha^{1/2}\|\boldsymbol{u} - \boldsymbol{u}_h\|_{0,K}$$
$$+ \nu^{1/2}h_K^{l_{\boldsymbol{u}}+1}|\boldsymbol{u}|_{l_{\boldsymbol{u}}+2,K} + \alpha^{1/2}h_K^{l_{\boldsymbol{u}}+2}|\boldsymbol{u}|_{l_{\boldsymbol{u}}+2,K} + \alpha^{1/2}\|\Pi_V \boldsymbol{u} - \boldsymbol{u}_h\|_{0,K}.$$

This inequality allows us to bound $|\boldsymbol{w}|_{1,K}$ in (3.10a) and (3.10b), obtaining (3.5b) and

$$\|\boldsymbol{u} - \boldsymbol{u}_h^*\|_{0,K} \preceq h_K^{l_{\boldsymbol{u}}+2}|\boldsymbol{u}|_{l_{\boldsymbol{u}}+2,K} + \|\Pi_V \boldsymbol{u} - \boldsymbol{u}_h\|_{0,K} + h_K\|\mathrm{L} - \mathrm{L}_h\|_{0,K}$$
$$+ (\alpha/\nu)^{1/2}h_K \left(\|\boldsymbol{u} - \boldsymbol{u}_h\|_{0,K} + \|\Pi_V \boldsymbol{u} - \boldsymbol{u}_h\|_{0,K} + h_K^{l_{\boldsymbol{u}}+2}|\boldsymbol{u}|_{l_{\boldsymbol{u}}+2,K}\right),$$

which implies (3.5a).

Finally, by trace inequality, we have $h_e\|\boldsymbol{v}\|_{0,e}^2 \preceq \|\boldsymbol{v}\|_{0,K}\left(\|\boldsymbol{v}\|_{0,K}^2 + h_K^2|\boldsymbol{v}|_{1,K}^2\right)^{1/2} \ \forall\, \boldsymbol{v} \in H^1(K)^d$. This implies

$$\sum_{e \in \mathscr{E}_h} h_e \|[\![\boldsymbol{u}_h^*]\!]\|_{0,e}^2 \preceq \sum_{e \in \mathscr{E}_h} \sum_{K' \in \omega_e} h_e \|\boldsymbol{u} - \boldsymbol{u}_h^*|_{K'}\|_{0,e}^2$$
$$\preceq \sum_{e \in \mathscr{E}_h} \sum_{K' \in \omega_e} \|\boldsymbol{u} - \boldsymbol{u}_h^*\|_{0,K'}\left(\|\boldsymbol{u} - \boldsymbol{u}_h^*\|_{0,K'}^2 + h_{K'}^2|\boldsymbol{u} - \boldsymbol{u}_h^*|_{1,K'}^2\right)^{1/2}$$

and (3.5c) follows. □

4. *A posteriori* error analysis

4.1   *Preliminaries*

We start by introducing estimates needed to prove our main results. First, in the next lemma, we state the approximation properties of the Clément interpolation operator $\mathscr{C}_h : L^1(\Omega) \to V_h^{1,c} \cap H_0^1(\Omega)$, introduced in Clément (1975), as

$$
\mathscr{C}_h w := \sum_{z \in \mathscr{N}_h^i} \left(\frac{1}{|\Omega_z|} \int_{\Omega_z} w \, \mathrm{d}x \right) \phi_z,
$$

where ϕ_z is the $\mathbb{P}_1$ nodal basis functions associated to the interior vertex z, $\Omega_z := \mathrm{supp}\,\phi_z$, $\mathscr{N}_h^i$ is the set of all the interior vertices and $V_h^{1,c} := \{w \in \mathscr{C}(\Omega) : w|_K \in \mathbb{P}_1(K), \ K \in \mathscr{T}_h\}$.

LEMMA 4.1   For any $K \in \mathscr{T}_h$, $e \in \mathscr{E}_h^i$ and $0 \leqslant m \leqslant 1$, the following estimates hold for any $w \in H_0^1(\Omega)$:

$$
\|\mathscr{C}_h w\|_{m,\Omega} \preceq \|w\|_{m,\Omega}, \quad \|w - \mathscr{C}_h w\|_{0,K} \preceq \theta_K \|\!| w |\!\|_{1,\Delta_K}, \quad \|w - \mathscr{C}_h w\|_{0,e} \preceq \nu^{-1/4} \theta_e^{1/2} \|\!| w |\!\|_{1,\Delta_e},
$$

where $\theta_S := \min\{h_S \nu^{-1/2}, \alpha^{-1/2}\}$, with S an element $K \in \mathscr{T}_h$ or a face $e \in \mathscr{E}_h$, $\Delta_K := \{K' \in \mathscr{T}_h : \overline{K'} \cap \overline{K} \neq \emptyset\}$ and $\Delta_e := \{K' \in \mathscr{T}_h : \overline{K'} \cap \overline{e} \neq \emptyset\}$.

Proof.   See Lemma 3.2 in Verfürth (1998).   □

The next result shows that an element w of V_h^* can be approximated by a continuous function $\widetilde{w} \in V_h^*$, its Oswald interpolation, and that the approximation error can be controlled by the size of the inter-element jumps of w.

LEMMA 4.2   Let D^γ be the row-wise gradient or identity operator (for $|\gamma| = 1$ or $|\gamma| = 0$, respectively). For any $w_h \in V_h^*$ and any multi-index γ with $|\gamma| = 0, 1$ the following approximation result holds: let g be the restriction to Γ of a function in $V_h^* \cap H^1(\Omega)^d$. Then there exists a function $\widetilde{w}_h \in V_h^* \cap H^1(\Omega)^d$ satisfying $\widetilde{w}_h|_\Gamma = g$ and

$$
\sum_{K \in \mathscr{T}_h} \|D^\gamma(w_h - \widetilde{w}_h)\|_{0,K}^2 \preceq \sum_{e \in \mathscr{E}_h^i} h_e^{1-2|\gamma|} \|[\![w_h]\!]\|_{0,e}^2 + \sum_{e \in \mathscr{E}_h^\partial} h_e^{1-2|\gamma|} \|g - w_h\|_{0,e}^2.
$$

Proof.   Apply Theorem 2.2 in Karakashian & Pascal (2003) to each component.   □

To avoid nonessential technical difficulties, we make the following assumption:

Assumption H: We assume that the Dirichlet boundary data u_D is the trace of a continuous function in V_h^* and f a piecewise polynomial function. Otherwise, high-order terms associated to oscillations involving u_D and f will appear.

Finally, in order to prove the local efficiency of the error estimator, we need to construct suitable local cut-off functions which will allow us to localize the error analysis. More precisely, let $B_K := \Pi_{i=1}^{d+1} \lambda_i$ be the element-bubble function associated to $K \in \mathscr{T}_h$, where $\{\lambda_i\}_{i=1}^{d+1}$ are the barycentric coordinates of K. We define the face-bubble function B_e associated to the face $e \subset \partial K$ as follows: let j be the index such that λ_j vanishes on e, then $B_e := \Pi_{\substack{i=1 \\ i \neq j}}^{d+1} \lambda_i$.

LEMMA 4.3 The following estimates hold for all $\boldsymbol{v} \in \mathbb{P}_k(K)^d$, $K \in \mathscr{T}_h$, $\boldsymbol{\mu} \in \mathbb{P}_k(e)^d$ and $e \in \mathscr{E}_h$:

$$\|\boldsymbol{v}\|_{0,K}^2 \preceq (\boldsymbol{v}, B_K \boldsymbol{v})_K, \qquad \|B_K \boldsymbol{v}\|_{0,K} \preceq \|\boldsymbol{v}\|_{0,K}, \qquad \|\!|B_K \boldsymbol{v}|\!\|_{1,K} \preceq \theta_K^{-1} \|\boldsymbol{v}\|_{0,K},$$

$$\|\boldsymbol{\mu}\|_{0,e}^2 \preceq (\boldsymbol{\mu}, B_e \boldsymbol{\mu})_e, \qquad \|B_e \boldsymbol{\mu}\|_{0,\omega_e} \preceq \nu^{1/4} \theta_e^{1/2} \|\boldsymbol{\mu}\|_{0,e}, \qquad \|\!|B_e \boldsymbol{\mu}|\!\|_{1,\omega_e} \preceq \nu^{1/4} \theta_e^{-1/2} \|\boldsymbol{\mu}\|_{0,e}.$$

Proof. The proof is an extension of Lemma 3.3 in Verfürth (1998). $\qquad\square$

4.2 A posteriori *error estimator*

For each $K \in \mathscr{T}_h$, we propose the following local error estimator

$$\eta_K^2 := \theta_K^2 \|\boldsymbol{f} + \nabla \cdot (\nu \mathrm{L}_h) - \nabla p_h - \alpha \boldsymbol{u}_h^*\|_{0,K}^2 + \nu \|\mathrm{L}_h - \nabla \boldsymbol{u}_h^*\|_{0,K}^2 + \nu \|\nabla \cdot \boldsymbol{u}_h^*\|_{0,K}^2 \tag{4.1}$$

$$+ \frac{1}{2} \sum_{e \in \mathscr{E}_h^i \cap \partial K} \left(\nu^{-1/2} \theta_e \|[\![\nu \mathrm{L}_h - p_h \mathrm{I}]\!]\|_{0,e}^2 + \nu h_e^{-1} \|[\![\boldsymbol{u}_h^*]\!]\|_{0,e}^2 \right) + \sum_{e \in \mathscr{E}_h^\partial \cap \partial K} \nu h_e^{-1} \|\boldsymbol{u}_D - \boldsymbol{u}_h^*\|_{0,e}^2$$

and its global version $\eta_h := \left(\sum_{K \in \mathscr{T}_h} \eta_K^2 \right)^{1/2}$. Here we recall that θ_K and θ_e were defined in Lemma 4.1 and $\boldsymbol{u}_h^*$ is the postprocessed solution constructed in (2.3).

Note that the three volumetric terms are the residuals associated to the equilibrium equation, the constitutive equation and the incompressibility condition, respectively. At the same time, the jumps across the faces allude to the continuity of the trace of $\boldsymbol{u}$ and the normal trace of $\nu \mathrm{L} - p\mathrm{I}$, in case of enough regularity of the continuous solution. The last term, which is not usual in *a posteriori* error estimates for Dirichlet problems, is a measure of the quality of the approximation of boundary condition. We will see that our estimator converges to zero with order of $\min\{\ell_\mathrm{L}, \ell_{\boldsymbol{u}}, \ell_\sigma\} + 1$ and, if L, $\boldsymbol{u}$ and p have enough regularity, with order $k + 1$.

Now, we present intermediate results that will allow us to prove our main theorems. We proceed with adapting and extending the techniques introduced in Cockburn *et al.* (2011) and Cockburn & Zhang (2012, 2013) to the Brinkman problem. We emphasize that we keep track the dependence on ν and α.

We start by showing two lemmas that will allow us to prove the reliability of our estimator.

LEMMA 4.4 Let $(\mathrm{L}, \boldsymbol{u}, p)$ be the solution of (1.1) and $(\mathrm{L}_h, \boldsymbol{u}_h, p_h, \widehat{\boldsymbol{u}}_h)$ the solution of (2.2). Then

$$\nu^{-1/2} \|p - p_h\|_{0,\mathscr{T}_h} \preceq C_{\alpha,\nu} \left\{ \nu^{1/2} \|\mathrm{L} - \mathrm{L}_h\|_{0,\mathscr{T}_h} + \alpha^{1/2} \|\boldsymbol{u} - \widetilde{\boldsymbol{u}}_h^*\|_{0,\mathscr{T}_h} + \alpha^{1/2} \|\boldsymbol{u}_h^* - \widetilde{\boldsymbol{u}}_h^*\|_{0,\mathscr{T}_h} \right.$$

$$+ \nu^{1/2} \|\mathrm{L}_h - \nabla \boldsymbol{u}_h^*\|_{0,\mathscr{T}_h} + \sum_{K \in \mathscr{T}_h} \left(\theta_K \|\boldsymbol{f} + \nabla \cdot (\nu \mathrm{L}_h) - \nabla p_h - \alpha \boldsymbol{u}_h^*\|_{0,K} + \frac{1}{2} \sum_{e \in \mathscr{E}_h^i \cap \partial K} \nu^{-1/4} \theta_e^{1/2} \|[\![\nu \mathrm{L}_h - p_h \mathrm{I}]\!]\|_{0,e} \right) \right\},$$

where $\widetilde{\boldsymbol{u}}_h^*$ is the Oswald interpolation of the postprocessed velocity $\boldsymbol{u}_h^*$ and $C_{\alpha,\nu} := \max\{1, (\alpha/\nu)^{1/2}\}$.

Proof. Note that, for $q \in L_0^2(\Omega)$, we have (Girault & Raviart, 1986, Chapter 1, Corollary 2.4)

$$\nu^{-1/2} \|q\|_{0,\mathscr{T}_h} \preceq \sup_{\boldsymbol{w} \in H_0^1(\Omega)^d \setminus \{\boldsymbol{0}\}} \frac{(q, \nabla \cdot \boldsymbol{w})_{\mathscr{T}_h}}{\nu^{1/2} \|\nabla \boldsymbol{w}\|_{0,\mathscr{T}_h}}.$$

We take $q = p - p_h$ which is in $L_0^2(\Omega)$ because of (1.1e) and (2.2f). Then, we use the above inf–sup condition estimate $\nu^{-1/2}\|p - p_h\|_{0,\mathscr{T}_h}$. More precisely, for $\boldsymbol{w} \in H_0^1(\Omega)^d$ we get

$$(p - p_h, \nabla \cdot \boldsymbol{w})_{\mathscr{T}_h} = -\nu(\nabla \cdot (\mathrm{L} - \mathrm{L}_h), \boldsymbol{w})_{\mathscr{T}_h} + \alpha(\boldsymbol{u} - \boldsymbol{u}_h^*, \boldsymbol{w})_{\mathscr{T}_h} - (\boldsymbol{f} + \nabla \cdot (\nu \mathrm{L}_h) - \nabla p_h - \alpha \boldsymbol{u}_h^*, \boldsymbol{w})_{\mathscr{T}_h}$$
$$+ \langle (p - p_h)\boldsymbol{n}, \boldsymbol{w}\rangle_{\partial\mathscr{T}_h}$$

after integrating by parts, by using (2.3a) and rearranging the expression. Then, using integration by parts and breaking the resulting boundary integral into face integrals, we arrive at

$$(p - p_h, \nabla \cdot \boldsymbol{w})_{\mathscr{T}_h} = \nu(\mathrm{L} - \mathrm{L}_h, \nabla \boldsymbol{w})_{\mathscr{T}_h} + \alpha(\boldsymbol{u} - \boldsymbol{u}_h^*, \boldsymbol{w})_{\mathscr{T}_h} - (\boldsymbol{f} + \nabla \cdot (\nu \mathrm{L}_h) - \nabla p_h - \alpha \boldsymbol{u}_h^*, (\mathrm{Id} - \mathscr{C}_h)\boldsymbol{w})_{\mathscr{T}_h}$$
$$+ \langle [\![\nu \mathrm{L}_h - p_h \mathrm{I}]\!], (\mathrm{Id} - \mathscr{C}_h)\boldsymbol{w}\rangle_{\mathscr{E}_h^i} + R,$$

where $R := -(\boldsymbol{f} + \nabla \cdot (\nu \mathrm{L}_h) - \nabla p_h - \alpha \boldsymbol{u}_h^*, \mathscr{C}_h \boldsymbol{w})_{\mathscr{T}_h} + \langle \nu \mathrm{L}_h \boldsymbol{n} - p_h \boldsymbol{n}, \mathscr{C}_h \boldsymbol{w}\rangle_{\partial\mathscr{T}_h}$.

On the other hand, after integrating by parts and using (2.3a), (2.2b) reads

$$(\boldsymbol{f} + \nabla \cdot (\nu \mathrm{L}_h) - \nabla p_h - \alpha \boldsymbol{u}_h^*, \boldsymbol{v})_{\mathscr{T}_h} + \nu(\mathrm{L}_h - \nabla \boldsymbol{u}_h^*, \nabla \boldsymbol{v})_{\mathscr{T}_h} = \langle \nu \mathrm{L}_h \boldsymbol{n} - p_h \boldsymbol{n}, \boldsymbol{v}\rangle_{\partial\mathscr{T}_h} - \langle \nu \widehat{\mathrm{L}}_h \boldsymbol{n} - \widehat{p}_h \boldsymbol{n}, \boldsymbol{v}\rangle_{\partial\mathscr{T}_h}$$

for all $\boldsymbol{v} \in V_h^{1,c} := \{\boldsymbol{v} \in H_0^1(\Omega)^d : \boldsymbol{v}|_K \in \mathbb{P}_1(K)^d \ \forall K \in \mathscr{T}_h\}$. Then, since $\boldsymbol{v}|_e \in \mathbb{P}_k(e)^d$ for all $e \in \mathscr{E}_h$ and using (2.2e), we get

$$(\boldsymbol{f} + \nabla \cdot (\nu \mathrm{L}_h) - \nabla p_h - \alpha \boldsymbol{u}_h^*, \boldsymbol{v})_{\mathscr{T}_h} + \nu(\mathrm{L}_h - \nabla \boldsymbol{u}_h^*, \nabla \boldsymbol{v})_{\mathscr{T}_h} = \langle \nu \mathrm{L}_h \boldsymbol{n} - p_h \boldsymbol{n}, \boldsymbol{v}\rangle_{\partial\mathscr{T}_h \setminus \Gamma} \quad \forall \boldsymbol{v} \in V_h^{1,c}. \quad (4.2)$$

Now, taking $\boldsymbol{v} := \mathscr{C}_h \boldsymbol{w} \in V_h^{1,c}$ and using (4.2), we see that $R = \nu\left(\mathrm{L}_h - \nabla \boldsymbol{u}_h^*, \nabla \mathscr{C}_h \boldsymbol{w}\right)_{\mathscr{T}_h}$. Thus,

$$(p - p_h, \nabla \cdot \boldsymbol{w})_{\mathscr{T}_h} \leqslant \nu\|\mathrm{L} - \mathrm{L}_h\|_{0,\mathscr{T}_h}\|\nabla \boldsymbol{w}\|_{0,\mathscr{T}_h}$$
$$+ \alpha\|\boldsymbol{u} - \boldsymbol{u}_h^*\|_{0,\mathscr{T}_h}\|\boldsymbol{w}\|_{0,\mathscr{T}_h} + \nu\|\mathrm{L}_h - \nabla \boldsymbol{u}_h^*\|_{0,\mathscr{T}_h}\|\nabla \mathscr{C}_h \boldsymbol{w}\|_{0,\mathscr{T}_h}$$
$$+ \|\boldsymbol{f} + \nabla \cdot (\nu \mathrm{L}_h) - \nabla p_h - \alpha \boldsymbol{u}_h^*\|_{0,\mathscr{T}_h}\|(\mathrm{Id} - \mathscr{C}_h)\boldsymbol{w}\|_{0,\mathscr{T}_h}$$
$$+ \|[\![\nu \mathrm{L}_h - p_h \mathrm{I}]\!]\|_{0,\mathscr{E}_h^i}\|(\mathrm{Id} - \mathscr{C}_h)\boldsymbol{w}\|_{0,\mathscr{E}_h^i}$$
$$\preceq C_{\alpha,\nu}\left\{\nu^{1/2}\|\mathrm{L} - \mathrm{L}_h\|_{0,\mathscr{T}_h} + \alpha^{1/2}\|\boldsymbol{u} - \widetilde{\boldsymbol{u}}_h^*\|_{0,\mathscr{T}_h} + \alpha^{1/2}\|\boldsymbol{u}_h^* - \widetilde{\boldsymbol{u}}_h^*\|_{0,\mathscr{T}_h} + \nu^{1/2}\|\mathrm{L}_h - \nabla \boldsymbol{u}_h^*\|_{0,\mathscr{T}_h}\right.$$
$$+ \sum_{K \in \mathscr{T}_h}\left(\theta_K\|\boldsymbol{f} + \nabla \cdot (\nu \mathrm{L}_h) - \nabla p_h - \alpha \boldsymbol{u}_h^*\|_{0,K} + \frac{1}{2}\sum_{e \in \mathscr{E}_h^i \cap \partial K}\nu^{-1/4}\theta_e^{1/2}\|[\![\nu \mathrm{L}_h - p_h \mathrm{I}]\!]\|_{0,e}\right)\right\}$$
$$\times \nu^{1/2}\|\nabla \boldsymbol{w}\|_{0,\Omega},$$

where we used the stability property of the Clément interpolator, Poincaré inequality, Lemma 4.1 and the regularity of the mesh. The result follows from dividing the above inequality by $\nu^{1/2}\|\nabla \boldsymbol{w}\|_{0,\Omega}$. $\quad\square$

LEMMA 4.5 Let $(L, \boldsymbol{u}, p)$ be the solution of (1.1) and $(L_h, \boldsymbol{u}_h, p_h, \widehat{\boldsymbol{u}}_h)$ the solution of (2.2). Then

$$\nu\|L - L_h\|_{0,\mathcal{T}_h}^2 + \alpha\|\boldsymbol{u} - \widetilde{\boldsymbol{u}}_h^*\|_{0,\mathcal{T}_h}^2 \preceq C_{\alpha,\nu}\left(\eta_h^2 + \nu\|\nabla(\boldsymbol{u}_h^* - \widetilde{\boldsymbol{u}}_h^*)\|_{0,\mathcal{T}_h}^2\right) + \alpha\|\boldsymbol{u}_h^* - \widetilde{\boldsymbol{u}}_h^*\|_{0,\mathcal{T}_h}^2.$$

Proof. Let $\widetilde{\boldsymbol{u}}_h^* \in H^1(\Omega)^d$ be the Oswald interpolation of $\boldsymbol{u}_h^*$. Using equations (1.1) and integrating by parts, we obtain

$$\begin{aligned}
\nu\|L - L_h\|_{0,\mathcal{T}_h}^2 + \alpha\|\boldsymbol{u} - \widetilde{\boldsymbol{u}}_h^*\|_{0,\mathcal{T}_h}^2 =&\, \nu(L - L_h, L - L_h)_{\mathcal{T}_h} + (\alpha(\boldsymbol{u} - \widetilde{\boldsymbol{u}}_h^*), \boldsymbol{u} - \widetilde{\boldsymbol{u}}_h^*)_{\mathcal{T}_h}\\
=&\, \nu(L - L_h, L - L_h)_{\mathcal{T}_h} + (\boldsymbol{f} + \nabla \cdot (\nu L_h) - \nabla p_h - \alpha\boldsymbol{u}_h^*, \boldsymbol{u} - \widetilde{\boldsymbol{u}}_h^*)_{\mathcal{T}_h}\\
&+ (\nabla \cdot \nu(L - L_h), \boldsymbol{u} - \widetilde{\boldsymbol{u}}_h^*)_{\mathcal{T}_h} - (\nabla(p - p_h), \boldsymbol{u} - \widetilde{\boldsymbol{u}}_h^*)_{\mathcal{T}_h}\\
&+ (\alpha(\boldsymbol{u}_h^* - \widetilde{\boldsymbol{u}}_h^*), \boldsymbol{u} - \widetilde{\boldsymbol{u}}_h^*)_{\mathcal{T}_h}.
\end{aligned}$$

Thus, after integrating by parts the third and fourth terms in previous expression and using the fact that $L = \nabla\boldsymbol{u}$, we write $\nu\|L - L_h\|_{0,\mathcal{T}_h}^2 + \alpha\|\boldsymbol{u} - \widetilde{\boldsymbol{u}}_h^*\|_{0,\mathcal{T}_h}^2 = \sum_{K \in \mathcal{T}_h} T_{1,K} + T_{2,K} + T_{3,K}$, where

$$T_{1,K} := (\boldsymbol{f} + \nabla \cdot (\nu L_h) - \nabla p_h - \alpha\boldsymbol{u}_h^*, \boldsymbol{u} - \widetilde{\boldsymbol{u}}_h^*)_K + \langle \nu(L - L_h)\boldsymbol{n}, \boldsymbol{u} - \widetilde{\boldsymbol{u}}_h^* \rangle_{\partial K \setminus \Gamma} - \langle (p - p_h)\boldsymbol{n}, \boldsymbol{u} - \widetilde{\boldsymbol{u}}_h^* \rangle_{\partial K \setminus \Gamma},$$

$$T_{2,K} := (p - p_h, \nabla \cdot (\boldsymbol{u} - \widetilde{\boldsymbol{u}}_h^*))_K \text{ and } T_{3,K} := -\nu(L - L_h, L_h - \nabla\widetilde{\boldsymbol{u}}_h^*)_K + \alpha(\boldsymbol{u} - \widetilde{\boldsymbol{u}}_h^*, \boldsymbol{u}_h^* - \widetilde{\boldsymbol{u}}_h^*)_{\mathcal{T}_h}.$$

Since $\boldsymbol{u} - \widetilde{\boldsymbol{u}}_h^* \in H_0^1(\Omega)^d$ (Lemma 4.2 with $\boldsymbol{g} = \boldsymbol{u}_D$), and $\nu L - pI \in H(\mathrm{div}, \Omega)^d$, we get

$$\sum_{K \in \mathcal{T}_h} T_{1,K} = (\boldsymbol{f} + \nabla \cdot (\nu L_h) - \nabla p_h - \alpha\boldsymbol{u}_h^*, (\mathsf{Id} - \mathscr{C}_h)(\boldsymbol{u} - \widetilde{\boldsymbol{u}}_h^*))_{\mathcal{T}_h} - \langle \nu L_h \boldsymbol{n} - p_h \boldsymbol{n}, (\mathsf{Id} - \mathscr{C}_h)(\boldsymbol{u} - \widetilde{\boldsymbol{u}}_h^*) \rangle_{\partial \mathcal{T}_h \setminus \Gamma} + T,$$

where $T := (\boldsymbol{f} + \nabla \cdot (\nu L_h) - \nabla p_h - \alpha\boldsymbol{u}_h^*, \mathscr{C}_h(\boldsymbol{u} - \widetilde{\boldsymbol{u}}_h^*))_{\mathcal{T}_h} - \langle L_h \boldsymbol{n} - p_h \boldsymbol{n}, \mathscr{C}_h(\boldsymbol{u} - \widetilde{\boldsymbol{u}}_h^*) \rangle_{\partial \mathcal{T}_h \setminus \Gamma}$.

Now, taking $w = \mathscr{C}_h(\boldsymbol{u} - \widetilde{\boldsymbol{u}}_h^*)$ in (4.2), we get $T = -\nu(L_h - \nabla\boldsymbol{u}_h^*, \nabla\mathscr{C}_h(\boldsymbol{u} - \widetilde{\boldsymbol{u}}_h^*))_{\mathcal{T}_h}$. Thus,

$$\begin{aligned}
\sum_{K \in \mathcal{T}_h} T_{1,K} =&\, (\boldsymbol{f} + \nabla \cdot (\nu L_h) - \nabla p_h - \alpha\boldsymbol{u}_h^*, (\mathsf{Id} - \mathscr{C}_h)(\boldsymbol{u} - \widetilde{\boldsymbol{u}}_h^*))_{\mathcal{T}_h}\\
&+ \langle [\![\nu L_h - p_h I]\!], (\mathsf{Id} - \mathscr{C}_h)(\boldsymbol{u} - \widetilde{\boldsymbol{u}}_h^*) \rangle_{\mathscr{E}_h^i} + T \preceq \sum_{K \in \mathcal{T}_h} \theta_K^2 \|\boldsymbol{f} + \nabla \cdot (\nu L_h) - \nabla p_h - \alpha\boldsymbol{u}_h^*\|_{0,K}^2\\
&+ \sum_{e \in \mathscr{E}_h^i} \nu^{-1/2}\theta_e \|[\![\nu L_h - p_h I]\!]\|_{0,e}^2 + \nu\|L_h - \nabla\boldsymbol{u}_h^*\|_{0,\mathcal{T}_h}^2\\
&+ \frac{1}{24}\left(\sum_{K \in \mathcal{T}_h} \theta_K^{-2}\|(\mathsf{Id} - \mathscr{C}_h)(\boldsymbol{u} - \widetilde{\boldsymbol{u}}_h^*)\|_{0,K}^2 + \sum_{e \in \mathscr{E}_h^i} \nu^{1/2}\theta_e^{-1}\|(\mathsf{Id} - \mathscr{C}_h)(\boldsymbol{u} - \widetilde{\boldsymbol{u}}_h^*)\|_{0,e}^2\right.\\
&\left.+ \nu\|\nabla\mathscr{C}_h(\boldsymbol{u} - \widetilde{\boldsymbol{u}}_h^*)\|_{0,\mathcal{T}_h}^2\right),
\end{aligned}$$

thanks to Cauchy–Schwarz and Young inequalities. Finally, using Lemma 4.1 and the regularity of the mesh, we get

$$
\sum_{K \in \mathcal{T}_h} T_{1,K} \preceq \sum_{K \in \mathcal{T}_h} \left(\theta_K^2 \| \boldsymbol{f} + \nabla \cdot (\nu \mathrm{L}_h) - \nabla p_h - \alpha \boldsymbol{u}_h^* \|_{0,K}^2 + \frac{1}{2} \sum_{e \in \mathcal{E}_h^i \cap \partial K} \nu^{-1/2} \theta_e \| [\![\nu \mathrm{L}_h - p_h \mathrm{I}]\!] \|_{0,e}^2 \right.
$$

$$
\left. + \nu \| \mathrm{L}_h - \nabla \boldsymbol{u}_h^* \|_{0,K}^2 \right) + \frac{1}{8} \| \boldsymbol{u} - \widetilde{\boldsymbol{u}}_h^* \|_{1,\mathcal{T}_h}^2. \tag{4.3}
$$

On the other hand, since $\boldsymbol{u}$ is divergence-free, we obtain

$$
\sum_{K \in \mathcal{T}_h} T_{2,K} = -(p - p_h, \nabla \cdot \widetilde{\boldsymbol{u}}_h^*)_{\mathcal{T}_h} \leqslant \frac{1}{12} C_{\alpha,\nu}^{-2} \nu^{-1} \| p - p_h \|_{0,\mathcal{T}_h}^2 + C_{\alpha,\nu}^2 \nu \| \nabla \cdot \widetilde{\boldsymbol{u}}_h^* \|_{0,\mathcal{T}_h}^2
$$

$$
\preceq \frac{1}{12} C_{\alpha,\nu}^{-2} \nu^{-1} \| p - p_h \|_{0,\mathcal{T}_h}^2 + C_{\alpha,\nu}^2 \nu \| \nabla (\boldsymbol{u}_h^* - \widetilde{\boldsymbol{u}}_h^*) \|_{0,\mathcal{T}_h}^2 + C_{\alpha,\nu}^2 \nu \| \nabla \cdot \boldsymbol{u}_h^* \|_{0,\mathcal{T}_h}^2. \tag{4.4}
$$

For the third term we have

$$
\sum_{K \in \mathcal{T}_h} T_{3,K} \leqslant \frac{1}{12} \nu \| \mathrm{L} - \mathrm{L}_h \|_{0,\mathcal{T}_h}^2 + \nu \| \mathrm{L}_h - \nabla \boldsymbol{u}_h^* \|_{0,\mathcal{T}_h}^2
$$

$$
+ \nu \| \nabla (\boldsymbol{u}_h^* - \widetilde{\boldsymbol{u}}_h^*) \|_{0,\mathcal{T}_h}^2 + \frac{5}{24} \alpha \| \boldsymbol{u} - \widetilde{\boldsymbol{u}}_h^* \|_{0,\mathcal{T}_h}^2 + \alpha \| \boldsymbol{u}_h^* - \widetilde{\boldsymbol{u}}_h^* \|_{0,\mathcal{T}_h}^2. \tag{4.5}
$$

Finally, using estimates (4.3)–(4.5), Lemma 4.4, the definitions of $\| \cdot \|_{1,\mathcal{T}_h}$ and η_h, we get

$$
\nu \| \mathrm{L} - \mathrm{L}_h \|_{0,\mathcal{T}_h}^2 + \alpha \| \boldsymbol{u} - \widetilde{\boldsymbol{u}}_h^* \|_{0,\mathcal{T}_h}^2
$$

$$
\preceq C_{\alpha,\nu}^2 \left(\eta_h^2 + \nu \| \nabla (\boldsymbol{u}_h^* - \widetilde{\boldsymbol{u}}_h^*) \|_{0,\mathcal{T}_h}^2 \right) + \alpha \| \boldsymbol{u}_h^* - \widetilde{\boldsymbol{u}}_h^* \|_{0,\mathcal{T}_h}^2 + \frac{1}{2} \left(\nu \| \mathrm{L} - \mathrm{L}_h \|_{0,\mathcal{T}_h}^2 + \alpha \| \boldsymbol{u} - \widetilde{\boldsymbol{u}}_h^* \|_{0,\mathcal{T}_h}^2 \right)
$$

and the result follows. $\qquad \square$

The next four lemmas provide us the tools to prove local efficiency of our estimator.

LEMMA 4.6 Let $e \in \mathcal{E}_h^i$, then

$$
\nu^{-1/2} \theta_e \| [\![\nu \mathrm{L}_h - p_h \mathrm{I}]\!] \|_{0,e}^2 \preceq \sum_{K \in \omega_e} \left(\nu \| \mathrm{L} - \mathrm{L}_h \|_{0,K}^2 + \nu^{-1} \| p - p_h \|_{0,K}^2 + \alpha \| \boldsymbol{u} - \boldsymbol{u}_h^* \|_{0,K}^2 \right.
$$

$$
\left. + \theta_K^2 \| \boldsymbol{f} + \nabla \cdot (\nu \mathrm{L}_h) - \nabla p_h - \alpha \boldsymbol{u}_h^* \|_{0,K}^2 \right).
$$

Proof. For any $\boldsymbol{v} \in H_0^1(\omega_e)^d$ we have

$$\langle [\![\nu L_h - p_h I]\!], \boldsymbol{v} \rangle_e = \sum_{K \in \omega_e} (\langle \nu(L_h - L)\boldsymbol{n}, \boldsymbol{v} \rangle_{\partial K} + \langle (p - p_h)\boldsymbol{n}, \boldsymbol{v} \rangle_{\partial K})$$

$$= \sum_{K \in \omega_e} ((\nu(L_h - L), \nabla \boldsymbol{v})_K + (\nu \nabla \cdot (L_h - L), \boldsymbol{v})_K + (\nabla(p - p_h), \boldsymbol{v})_K + (p - p_h, \nabla \cdot \boldsymbol{v})_K)$$

$$= \sum_{K \in \omega_e} ((\nu(L_h - L), \nabla \boldsymbol{v})_K + (p - p_h, \nabla \cdot \boldsymbol{v})_K + (\alpha(\boldsymbol{u} - \boldsymbol{u}_h^*), \boldsymbol{v})_K + (\boldsymbol{f} + \nabla \cdot (\nu L_h) - \nabla p_h - \alpha \boldsymbol{u}_h^*, \boldsymbol{v})_K)$$

$$\leqslant \sum_{K \in \omega_e} \left(\nu^{1/2} \|L - L_h\|_{0,K} + \nu^{-1/2} \|p - p_h\|_{0,K} + \alpha^{1/2} \|\boldsymbol{u} - \boldsymbol{u}_h^*\|_{0,K} + \theta_K \|\boldsymbol{f} + \nabla \cdot (\nu L_h) - \nabla p_h - \alpha \boldsymbol{u}_h^*\|_{0,K} \right) T_{\boldsymbol{v}},$$

where $T_{\boldsymbol{v}} := \nu^{1/2} \|\nabla \boldsymbol{v}\|_{0,K} + \nu^{1/2} \|\nabla \cdot \boldsymbol{v}\|_{0,K} + \alpha^{1/2} \|\boldsymbol{v}\|_{0,K} + \theta_K^{-1} \|\boldsymbol{v}\|_{0,K}$.

On the other hand, taking $\boldsymbol{v} := B_e [\![\nu L_h - p_h I]\!]$ and applying Lemma 4.3, we get

$$T_{\boldsymbol{v}} \preceq \|\boldsymbol{v}\|_{1,K} + \theta_e^{-1} \|\boldsymbol{v}\|_{0,K} \preceq \nu^{1/4} \theta_e^{-1/2} \|[\![\nu L_h - p_h I]\!]\|_{0,e}.$$

Thus, the result follows from Lemma 4.3 and the shape-regularity assumption. $\qquad\square$

LEMMA 4.7 For any element $K \in \mathscr{T}_h$ we have

$$\theta_K \|\boldsymbol{f} + \nabla \cdot (\nu L_h) - \nabla p_h - \alpha \boldsymbol{u}_h^*\|_{0,K} \preceq \nu^{1/2} \|L - L_h\|_{0,K} + \alpha^{1/2} \|\boldsymbol{u} - \boldsymbol{u}_h^*\|_{0,K} + \nu^{-1/2} \|p - p_h\|_{0,K}.$$

Proof. Let $\boldsymbol{v} = \boldsymbol{f} + \nabla \cdot (\nu L_h) - \nabla p_h - \alpha \boldsymbol{u}_h^*$ then, using (1.1b), the definition of B_K and integration by parts, we get

$$(\boldsymbol{v}, B_K \boldsymbol{v})_K = -\nu(\nabla \cdot (L - L_h), B_K \boldsymbol{v})_K + (\nabla(p - p_h), B_K \boldsymbol{v})_K + \alpha(\boldsymbol{u} - \boldsymbol{u}_h^*, B_K \boldsymbol{v})_K$$

$$= \nu(L - L_h, \nabla B_K \boldsymbol{v})_K - (p - p_h, \nabla \cdot B_K \boldsymbol{v})_K + \alpha(\boldsymbol{u} - \boldsymbol{u}_h^*, B_K \boldsymbol{v})_K$$

$$\preceq (\nu^{1/2} \|L - L_h\|_{0,K} + \nu^{-1/2} \|p - p_h\|_{0,K} + \alpha^{1/2} \|\boldsymbol{u} - \boldsymbol{u}_h^*\|_{0,K}) \|B_K \boldsymbol{v}\|_{1,K}.$$

Thus, the result follows from Lemma 4.3. $\qquad\square$

Now, note that to prove an upper bounds for the jump of the postprocessed velocity, we will use the decomposition of $\nu h_e^{-1} \|[\![\boldsymbol{u}_h^*]\!]\|_{0,e}^2$ into $\nu h_e^{-1} \|P_{M_0}[\![\boldsymbol{u}_h^*]\!]\|_{0,e}^2$ and $\nu h_e^{-1} \|(Id - P_{M_0})[\![\boldsymbol{u}_h^*]\!]\|_{0,e}^2$, where P_{M_0} is the L^2-orthogonal projection into

$$M_{0,h} := \{\boldsymbol{\mu} \in L^2(\mathscr{E}_h)^d : \boldsymbol{\mu}|_e \in \mathbb{P}_0(e)^d \quad \forall e \in \mathscr{E}_h\}.$$

LEMMA 4.8 For each face $e \in \mathscr{E}_h$ we have that $h_e^{-1} \|P_{M_0}[\![\boldsymbol{u}_h^*]\!]\|_{0,e}^2 \preceq \|L_h - \nabla \boldsymbol{u}_h^*\|_{0,\omega_e}^2$.

Proof. Let G be a tensor-valued function with rows in $RT_0(K)$ and set $\boldsymbol{w} := \nabla \cdot G \in \mathbb{P}_0(K)^d$. Then, from (2.3a) (or (2.3b) if $\alpha = 0$) we get that (2.2a) can be written as

$$(L_h, G)_K + (\boldsymbol{u}_h^*, \nabla \cdot G)_K = \langle \widehat{\boldsymbol{u}}_h, G\boldsymbol{n} \rangle_{\partial K}.$$

Thus, integrating by parts, we arrive at $(L_h - \nabla \boldsymbol{u}_h^*, G)_K = \langle \widehat{\boldsymbol{u}}_h - \boldsymbol{u}_h^*, G\boldsymbol{n} \rangle_{\partial K}$. For the rest of the proof we refer to Lemma 3.4 in Cockburn & Zhang (2014), adapted to vector-valued functions. $\qquad\square$

Now, for the remaining term in the decomposition of $\nu h_e^{-1} \| [\![\boldsymbol{u}_h^*]\!] \|_{0,e}^2$, we have the following estimate.

LEMMA 4.9 For each face $e \in \mathscr{E}_h$, $h_e^{-1} \| (\mathsf{Id} - \mathsf{P}_{\mathsf{M}_0}) [\![\boldsymbol{u}_h^*]\!] \|_{0,e}^2 \preceq \| \nabla(\boldsymbol{u} - \boldsymbol{u}_h^*) \|_{0,\omega_e}^2$.

Proof. See Lemma 3.5 in Cockburn & Zhang (2014). $\qquad\square$

4.3 *The main results*

For each $K \in \mathscr{T}_h$ we define the local error

$$\mathsf{e}_K^2 := \nu \| L - L_h \|_{0,K}^2 + \alpha \| \boldsymbol{u} - \boldsymbol{u}_h^* \|_{0,K}^2 + \nu \| \nabla(\boldsymbol{u} - \boldsymbol{u}_h^*) \|_{0,K}^2 + \nu^{-1} \| p - p_h \|_{0,K}^2, \qquad (4.6)$$

and its global version is given by $\mathsf{e}_h := \left(\sum_{K \in \mathscr{T}_h} \mathsf{e}_K^2 \right)^{1/2}$.

Now, we can state and prove the reliability and efficiency results for our *a posteriori* error estimator.

THEOREM 4.10 (Reliability).

$$\mathsf{e}_h \preceq C_{\alpha,\nu} \left(\eta_h + \sum_{e \in \mathscr{E}_h} \nu^{1/2} h_e^{1/2} \| [\![\boldsymbol{u}_h^*]\!] \|_{0,e} \right).$$

Proof. Thanks to Lemmas 4.4, 4.5 and the fact that, for each $K \in \mathscr{T}_h$, $\nu^{1/2} \| \nabla(\boldsymbol{u} - \boldsymbol{u}_h^*) \|_{0,K} \preceq \nu^{1/2} \| L - L_h \|_{0,K} + \eta_K$, we get

$$\nu \| L - L_h \|_{0,\mathscr{T}_h}^2 + \| \boldsymbol{u} - \boldsymbol{u}_h^* \|_{1,\mathscr{T}_h}^2 + \nu^{-1} \| p - p_h \|_{0,\mathscr{T}_h}^2 \preceq C_{\alpha,\nu} \left(\eta_h^2 + \nu \| \nabla(\boldsymbol{u}_h^* - \widetilde{\boldsymbol{u}}_h^*) \|_{0,\mathscr{T}_h}^2 + \alpha \| (\boldsymbol{u}_h^* - \widetilde{\boldsymbol{u}}_h^*) \|_{0,\mathscr{T}_h}^2 \right).$$

The result follows from Lemma 4.2, taking $\boldsymbol{w}_h = \boldsymbol{u}_h^*$ to bound the second and third terms on the right-hand side and the definition of $C_{\alpha,\nu}$. $\qquad\square$

REMARK 4.11 Note that if $\alpha = 0$ (Stokes problem), then $C_{\alpha,\nu} = 1$. Thus, to obtain an estimate for the L^2 norm of the error of the velocity, we proceed as follows

$$\begin{aligned}
\nu^{1/2} \| \boldsymbol{u} - \boldsymbol{u}_h^* \|_{0,\mathscr{T}_h} &\leqslant \nu^{1/2} \| \boldsymbol{u} - \widetilde{\boldsymbol{u}}_h^* \|_{0,\mathscr{T}_h} + \nu^{1/2} \| \boldsymbol{u}_h^* - \widetilde{\boldsymbol{u}}_h^* \|_{0,\mathscr{T}_h} \\
&\preceq \nu^{1/2} \| \nabla(\boldsymbol{u} - \widetilde{\boldsymbol{u}}_h^*) \|_{0,\mathscr{T}_h} + \sum_{e \in \mathscr{E}_h} \nu^{1/2} h_e^{1/2} \| [\![\boldsymbol{u}_h^*]\!] \|_{0,e} \preceq \eta_h + \sum_{e \in \mathscr{E}_h} \nu^{1/2} h_e^{1/2} \| [\![\boldsymbol{u}_h^*]\!] \|_{0,e},
\end{aligned}$$

thanks to Poincaré inequality, Lemma 4.2 and the bound for $\nu^{1/2} \| \nabla(\boldsymbol{u} - \widetilde{\boldsymbol{u}}_h^*) \|_{0,\mathscr{T}_h}$ from Theorem 4.10.

THEOREM 4.12 (Efficiency). Let $K \in \mathscr{T}_h$ and $\omega_K := \{ K' \in \mathscr{T}_h : K' \in \omega_e \text{ and } e \in \mathscr{E}_h \cap \partial K \}$, then

$$\eta_K \preceq \mathsf{e}_{\omega_K}.$$

Proof. By definition of η_K, Lemmas 4.6–4.9 and the inequalities $\|L_h - \nabla u_h^*\|_{0,K} \leqslant \|L - L_h\|_{0,K} + \|\nabla(u - u_h^*)\|_{0,K}$ and $\|\nabla \cdot u_h^*\|_{0,K} = \|\nabla \cdot (u - u_h^*)\|_{0,K} \preceq \|\nabla(u - u_h^*)\|_{0,K}$, we have that

$$
\begin{aligned}
\eta_K^2 &\preceq \nu\|L - L_h\|_{0,K}^2 + \alpha\|u - u_h^*\|_{0,K}^2 + \nu^{-1}\|p - p_h\|_{0,K}^2 + \nu\|L_h - \nabla u_h^*\|_{0,K}^2 \\
&\quad + \nu\|\nabla \cdot u_h^*\|_{0,K}^2 + \nu\|L - L_h\|_{0,\omega_K}^2 + \nu^{-1}\|p - p_h\|_{0,\omega_K}^2 \\
&\quad + \sum_{K' \in \omega_K} \theta_{K'}^2 \|f + \nabla \cdot (\nu L_h) - \nabla p_h - \alpha u_h^*\|_{0,K'}^2 + \nu\|\nabla(u - u_h^*)\|_{0,\omega_K}^2 + \nu\|L_h - \nabla u_h^*\|_{0,\omega_K}^2 \\
&\preceq \nu\|L - L_h\|_{0,\omega_K}^2 + |\!|\!| u - u_h^* |\!|\!|_{1,\omega_K}^2 + \nu^{-1}\|p - p_h\|_{0,\omega_K}^2,
\end{aligned}
$$

and the result follows. □

REMARK 4.13 Using (3.5c) and assuming enough regularity on L, u and p, we can see that the term $\sum_{e \in \mathscr{E}_h} \nu^{1/2} h_e^{1/2} \|[\![u_h^*]\!]\|_{0,e}$ is a high-order term. Its order of convergence is $\min\{\ell_u, \ell_L, \ell_\sigma\} + 2$ while the one associated to the estimator and the error is $\min\{\ell_u, \ell_L, \ell_\sigma\} + 1$.

5. Numerical experiments

In this section, we provide numerical simulations, for $d = 2$, illustrating the performance of the scheme and validating our main results in Theorems 4.10 and 4.12. In all the examples we consider different values of the polynomial degree ($k = 1$, 2 and 3), and set the stabilization parameter τ to be 1 on each edge. The values of the physical parameters α and ν will be specified on each example.

Let us define the errors $e_L := \nu^{1/2}\|L - L_h\|_{0,\mathscr{T}_h}$, $e_u := |\!|\!| u - u_h^* |\!|\!|_{1,\mathscr{T}_h}$, $e_p := \nu^{-1/2}\|p - p_h\|_{0,\mathscr{T}_h}$, the estimator terms η_i ($i = 1, \ldots, 5$)

$$
\eta_1^2 := \sum_{K \in \mathscr{T}_h} \theta_K^2 \|f + \nabla \cdot (\nu L_h) - \nabla p_h - \alpha u_h^*\|_{0,K}^2, \quad \eta_2^2 := \nu\|L_h - \nabla u_h^*\|_{0,\mathscr{T}_h}^2, \quad \eta_3^2 := \nu\|\nabla \cdot u_h^*\|_{0,\mathscr{T}_h}^2
$$

$$
\eta_4^2 := \nu^{-1/2}\sum_{e \in \mathscr{E}_h} \theta_e \|[\![\nu L_h - p_h I]\!]\|_{0,e}^2 \text{ and } \eta_5^2 := \nu \sum_{e \in \mathscr{E}_h} h_e^{-1}\|[\![u_h^*]\!]\|_{0,e}^2,
$$

and the effectivity index $\mathsf{eff} := \eta_h/e_h$. In some tables, we include a column *h.o.t.*, showing that the term defined in Remark 4.13 is in fact a high-order term, and thus it is not necessary to include it in the definition of our error estimator. The orders of convergence will be computed in terms of the number of elements N and we will use the fact that $h \simeq N^{-1/2}$.

For the tests that include adaptivity, we use the strategy given by the following:

   (i) Start with a coarse mesh $\mathscr{T}_h$.

   (ii) Solve the discrete problem on the current mesh $\mathscr{T}_h$.

   (iii) Compute η_K for each $K \in \mathscr{T}_h$.

   (iv) Use *red–blue–green* (for details, see Verfürth, 2013) procedure to refine each $K' \in \mathscr{T}_h$ such that $\eta_{K'} \geqslant \theta \max_{K \in \mathscr{T}_h} \eta_K$, with $\theta \in [0, 1]$.

   (v) Consider this new mesh as $\mathscr{T}_h$ and, unless a prescribed stopping criteria is satisfied, go to (ii).

TABLE 1 *History of convergence of the error terms for the Example 5.1 ($\nu = 1$)*

k	N	e_L	order	e_u	order	e_p	order
	16	9.13e-03	—	1.09e-02	—	7.29e-03	—
	64	2.41e-03	1.92	2.84e-03	1.94	1.75e-03	2.05
1	256	6.22e-04	1.96	7.29e-04	1.96	4.19e-04	2.06
	1024	1.58e-04	1.98	1.85e-04	1.98	1.02e-04	2.04
	4096	3.99e-05	1.99	4.66e-05	1.99	2.52e-05	2.02
	16384	1.00e-05	1.99	1.17e-05	1.99	6.27e-06	2.01
	16	9.40e-04	—	9.80e-04	—	5.10e-04	—
	64	1.14e-04	3.04	1.19e-04	3.04	6.09e-05	3.06
2	256	1.40e-05	3.02	1.46e-05	3.02	7.46e-06	3.03
	1024	1.74e-06	3.01	1.81e-06	3.01	9.21e-07	3.02
	4096	2.17e-07	3.01	2.26e-07	3.01	1.14e-07	3.01
	16384	2.70e-08	3.00	2.81e-08	3.00	1.42e-08	3.00
	16	1.63e-05	—	1.61e-05	—	1.69e-05	—
	64	1.05e-06	3.95	1.03e-06	3.97	1.03e-06	4.04
3	256	6.65e-08	3.98	6.50e-08	3.99	6.33e-08	4.02
	1024	4.18e-09	3.99	4.08e-09	3.99	3.93e-09	4.01
	4096	2.62e-10	4.00	2.55e-10	4.00	2.45e-10	4.00
	16384	1.64e-11	4.00	1.60e-11	4.00	1.53e-11	4.00

5.1 A polynomial solution

For this test case, we choose $\alpha = 1$ and $\Omega =]0, 1[\times]0, 1[$. The source term f and the boundary data u_D are chosen such that the exact solution of the problem is given by $u := (u_1, u_2)$, where $u_1(x_1, x_2) := x_1(1 - x_1)x_2(1 - x_2)$ and $u_2(x_1, x_2) := (2x_1 - 1)x_2^2(\frac{1}{2} - \frac{x_2}{3})$, and $p(x_1, x_2) := x_1^2 x_2^2 - \frac{1}{9}$. We note that f and u_D satisfy Assumption H when $k \geqslant 3$.

Table 1 shows the history of convergence of the error of each variable when the number of elements N quadruplicates, i.e. the mesh size h decreases by a factor two. We see that all the error terms converge with optimal order of $k + 1$, exactly as the error estimates in Section 3 predicted. In addition, we see in Table 2 that each term of the error estimator converges with the optimal order $k + 1$ and the high-order term with order $k + 2$.

We repeat the experiment considering now $\nu = 10^{-2}$. As Tables 3–4 show, similar conclusions can be drawn regarding the optimal order of convergence of the error and the estimator. The last column of Tables 2 and 4 displays the effectivity index. It remains bounded for each polynomial degree k, however, it increases with k. This is natural to expect since some of the constants on the estimates depend on k.

On the other hand, we observe in all the cases that the first term of the estimator (η_1) is larger than the other terms. This behavior, together with the fact that the effectivity index is larger than one, might suggest that the estimator is locating regions where the divergence of $\nu(L - L_h) + (p - p_h)I$ is large. Motivated by this issue, if we assume that the solution of the Brinkman problem is such that $L \in H(\text{div}, \Omega)^d$ and $p \in H^1(\Omega)$, we can add the term $\theta_K \|\nabla \cdot (\nu L - pI) - \nabla \cdot (\nu L_h - p_h I)\|_{0,K}$ to error e_K defined (4.6). Table 5 shows the behavior of the global estimator and the global error that includes the aforementioned term. In this case, we observe that effectivity index is close to 1.

In summary, this example shows that, even though $u_D \notin V_h^*$, as in the case of $k = 1$ and 2, Tables 1–5 verify that our error estimate is reliable and locally efficient as stated in Theorems 4.10 and 4.12.

TABLE 2 *History of convergence of the terms composing the error estimator for the Example 5.1 ($\nu = 1$)*

k	N	η_1	order	η_2	order	η_3	order	η_4	order	η_5	order	*h.o.t.*	order	eff
	16	1.49e-01	–	8.82e-03	–	6.16e-03	–	4.17e-02	–	7.26e-03	–	3.06e-03	–	9.734
	64	3.66e-02	2.03	2.30e-03	1.94	1.58e-03	1.96	1.06e-02	1.97	1.93e-03	1.92	4.14e-04	2.88	9.293
1	256	9.11e-03	2.01	5.76e-04	2.00	3.95e-04	2.00	2.73e-03	1.96	5.03e-04	1.94	5.51e-05	2.91	9.128
	1024	2.27e-03	2.00	1.43e-04	2.01	9.80e-05	2.01	6.96e-04	1.97	1.29e-04	1.96	7.13e-06	2.95	9.048
	4096	5.68e-04	2.00	3.56e-05	2.01	2.44e-05	2.01	1.76e-04	1.98	3.27e-05	1.98	9.08e-07	2.97	9.007
	16384	1.42e-04	2.00	8.88e-06	2.00	6.08e-06	2.00	4.42e-05	1.99	8.23e-06	1.99	1.15e-07	2.99	8.986
	16	1.86e-02	–	8.61e-04	–	6.78e-04	–	4.31e-03	–	3.97e-04	–	1.77e-04	–	13.214
	64	2.32e-03	3.01	1.08e-04	3.00	8.65e-05	2.97	5.76e-04	2.91	5.26e-05	2.91	1.18e-05	3.91	13.612
2	256	2.89e-04	3.00	1.34e-05	3.00	1.09e-05	2.99	7.44e-05	2.95	6.76e-06	2.96	7.58e-07	3.96	13.847
	1024	3.61e-05	3.00	1.68e-06	3.00	1.36e-06	3.00	9.47e-06	2.98	8.55e-07	2.98	4.80e-08	3.98	13.977
	4096	4.51e-06	3.00	2.10e-07	3.00	1.71e-07	3.00	1.19e-06	2.99	1.08e-07	2.99	3.02e-09	3.99	14.046
	16384	5.64e-07	3.00	2.62e-08	3.00	2.14e-08	3.00	1.50e-07	2.99	1.35e-08	3.00	1.89e-10	4.00	14.081
	16	6.54e-04	–	1.41e-05	–	7.02e-06	–	1.27e-04	–	2.97e-06	–	1.24e-06	–	23.429
	64	4.11e-05	3.99	8.80e-07	4.00	4.36e-07	4.01	8.51e-06	3.90	1.85e-07	4.01	3.80e-08	5.03	23.437
3	256	2.58e-06	4.00	5.51e-08	4.00	2.72e-08	4.00	5.49e-07	3.96	1.15e-08	4.01	1.17e-09	5.02	23.458
	1024	1.62e-07	4.00	3.45e-09	4.00	1.70e-09	4.00	3.48e-08	3.98	7.18e-10	4.00	3.62e-11	5.01	23.473
	4096	1.01e-08	4.00	2.16e-10	4.00	1.07e-10	4.00	2.19e-09	3.99	4.48e-11	4.00	1.12e-12	5.01	23.482
	16384	6.32e-10	4.00	1.35e-11	4.00	6.68e-12	4.00	1.37e-10	3.99	2.80e-12	4.00	3.50e-14	5.01	23.466

TABLE 3 *History of convergence of the error terms for the Example* 5.1 ($\nu = 10^{-2}$)

k	N	e_L	order	e_u	order	e_p	order
	16	2.89e-02	—	9.35e-02	—	6.55e-02	—
	64	1.09e-02	1.41	2.43e-02	1.94	1.47e-02	2.16
1	256	3.09e-03	1.82	5.12e-03	2.25	3.35e-03	2.13
	1024	8.22e-04	1.91	1.05e-03	2.29	7.43e-04	2.17
	4096	2.14e-04	1.94	2.32e-04	2.17	1.68e-04	2.15
	16384	5.51e-05	1.96	5.56e-05	2.06	3.93e-05	2.09
	16	2.06e-03	—	4.70e-03	—	5.73e-03	—
	64	3.16e-04	2.71	4.96e-04	3.25	6.46e-04	3.15
2	256	4.07e-05	2.96	4.89e-05	3.34	6.95e-05	3.22
	1024	5.01e-06	3.02	5.12e-06	3.26	7.61e-06	3.19
	4096	6.21e-07	3.01	5.86e-07	3.13	8.66e-07	3.14
	16384	7.76e-08	3.00	7.10e-08	3.05	1.02e-07	3.08
	16	7.83e-05	—	1.06e-04	—	1.83e-04	—
	64	5.14e-06	3.93	5.64e-06	4.23	9.97e-06	4.19
3	256	3.22e-07	4.00	3.01e-07	4.23	5.60e-07	4.16
	1024	2.03e-08	3.99	1.70e-08	4.14	3.25e-08	4.11
	4096	1.29e-09	3.98	1.01e-09	4.07	1.94e-09	4.07
	16384	8.12e-11	3.99	6.22e-11	4.03	1.18e-10	4.04

Moreover, the estimator is robust in the sense that the upper and lower bounds of error are uniformly bounded with respect to the physical parameters α and ν.

5.2 *The Kovasznay flow*

We set $\Omega = \,]0, 2[\, \times \,]{-}0.5, 1.5[$ and consider the Stokes problem ($\alpha = 0$) whose exact solution coincides with the analytical solution of the two-dimensional incompressible Navier–Stokes equations presented in Kovasznay (1948): $\boldsymbol{u} := (u_1, u_2)$, where $u_1(x_1, x_2) = 1 - \exp(\lambda x_1) \cos(2\pi x_2)$ and $u_2(x_1, x_2) = \frac{\lambda}{2\pi} \exp(\lambda x_1) \sin(2\pi x_2)$, and $p(x_1, x_2) = \frac{1}{2} \exp(2\lambda x_1) - \frac{\exp(4\lambda) - 1}{8\lambda}$. Here $\lambda = \frac{Re}{2} - \sqrt{\frac{Re^2}{4} + 4\pi^2}$ and $Re = \frac{1}{\nu}$. This is also a solution of our problem with $\boldsymbol{f} = -(\boldsymbol{u} \cdot \nabla)\boldsymbol{u}$ and $\boldsymbol{u}_D = \boldsymbol{u}|_\Gamma$.

Figure 1 depicts the error e_h (defined in (4.6)) versus the number of elements N, using uniform and adaptive ($\theta = 0.25$) refinements. Since the solution is smooth, we can see that the curves associated to uniform and adaptive refinements display the same order of convergence predicted by the theory, i.e order $N^{-(k+1)/2}$. In addition, we observe that the adaptive strategy is able to provide errors with the same magnitude as the uniform refinement, but with fewer elements.

5.3 *A singularly perturbed problem*

We set $\nu = 0.01$ and $\alpha = 1$. The domain is the unit square $\Omega = \,]0, 1[\times]0, 1[$, and $\boldsymbol{f}, \boldsymbol{u}_D$ are such that the exact solution is $\boldsymbol{u} := (u_1, u_2)$, where $u_1(x_1, x_2) = x_2 - \frac{1 - \exp(x_2/\nu)}{1 - \exp(1/\nu)}$ and $u_2(x_1, x_2) = x_1 - \frac{1 - \exp(x_1/\nu)}{1 - \exp(1/\nu)}$, and $p(x_1, x_2) = x_1 - x_2$. This solution has boundary layers at $x_1 = 1$ and $x_2 = 1$. In Fig. 2, we present the orders of convergence for e_h using uniform and adaptive refinements, for $k = 1, 2, 3$. We recover the predicted rates of convergence, up to an expected loss of convergence on very coarse meshes due

TABLE 4 *History of convergence of the terms composing the error estimator for the Example 5.1 ($\nu = 10^{-2}$)*

k	N	η_1	order	η_2	order	η_3	order	η_4	order	η_5	order	h.o.t.	order	eff
1	16	1.29e-01	–	7.20e-02	–	5.26e-02	–	3.96e-02	–	5.90e-02	–	2.47e-02	–	1.463
	64	8.55e-02	0.60	2.26e-02	1.67	1.67e-02	1.65	2.22e-02	0.84	1.78e-02	1.73	3.61e-03	2.77	3.106
	256	4.64e-02	0.88	4.96e-03	2.19	3.72e-03	2.17	1.01e-02	1.14	3.68e-03	2.28	3.68e-04	3.29	7.011
	1024	1.48e-02	1.65	9.76e-04	2.35	7.22e-04	2.37	3.28e-03	1.62	6.95e-04	2.40	3.56e-05	3.37	9.971
	4096	3.70e-03	2.00	2.05e-04	2.25	1.42e-04	2.35	9.30e-04	1.82	1.47e-04	2.25	3.87e-06	3.20	10.706
	16384	9.26e-04	2.00	4.77e-05	2.10	3.03e-05	2.23	2.50e-04	1.90	3.50e-05	2.07	4.69e-07	3.05	10.971
2	16	1.74e-02	–	5.02e-03	–	3.31e-03	–	4.02e-03	–	2.62e-03	–	1.13e-03	–	2.471
	64	4.70e-03	1.89	5.89e-04	3.09	3.91e-04	3.08	9.63e-04	2.06	3.02e-04	3.12	6.42e-05	4.13	5.567
	256	1.20e-03	1.97	6.30e-05	3.22	4.20e-05	3.22	1.99e-04	2.28	2.95e-05	3.35	3.13e-06	4.36	12.947
	1024	1.89e-04	2.67	7.07e-06	3.16	4.54e-06	3.21	2.94e-05	2.76	2.95e-06	3.32	1.56e-07	4.33	18.355
	4096	2.38e-05	2.99	8.49e-07	3.06	5.16e-07	3.14	4.00e-06	2.88	3.28e-07	3.17	8.63e-09	4.17	19.841
	16384	2.98e-06	3.00	1.06e-07	3.01	6.12e-08	3.08	5.23e-07	2.93	3.95e-08	3.06	5.17e-10	4.06	20.642
3	16	7.99e-04	–	1.34e-04	–	7.70e-05	–	1.41e-04	–	4.40e-05	–	1.87e-05	–	3.673
	64	1.04e-04	2.95	7.49e-06	4.16	3.55e-06	4.44	1.63e-05	3.11	2.25e-06	4.29	4.70e-07	5.31	8.375
	256	1.32e-05	2.97	4.31e-07	4.12	1.46e-07	4.60	1.66e-06	3.30	1.14e-07	4.30	1.13e-08	5.37	18.684
	1024	1.05e-06	3.66	2.64e-08	4.03	6.26e-09	4.54	1.21e-07	3.77	6.25e-09	4.19	2.95e-10	5.27	25.119
	4096	6.59e-08	3.99	1.66e-09	3.99	3.31e-10	4.24	8.09e-09	3.90	3.71e-10	4.08	8.47e-12	5.12	26.171
	16384	4.14e-09	3.99	1.05e-10	3.98	2.04e-11	4.02	5.24e-10	3.95	2.28e-11	4.02	2.58e-13	5.04	26.719

TABLE 5 *History of convergence of the modified global error and estimator for the Example 5.1 with $\nu = 1$ (left) and $\nu = 10^{-2}$ (right)*

| k	N	e_h	order	η_h	order	eff
	16	1.60e-02	—	1.56e-01	—	1.036
	64	4.12e-03	1.96	3.83e-02	2.02	1.039
1	256	1.05e-03	1.98	9.55e-03	2.00	1.041
	1024	2.64e-04	1.99	2.39e-03	2.00	1.043
	4096	6.63e-05	1.99	5.97e-04	2.00	1.044
	16384	1.66e-05	2.00	1.49e-04	2.00	1.044
	16	1.45e-03	—	1.92e-02	—	1.026
	64	1.76e-04	3.05	2.39e-03	3.00	1.030
2	256	2.16e-05	3.02	2.99e-04	3.00	1.032
	1024	2.68e-06	3.01	3.74e-05	3.00	1.033
	4096	3.33e-07	3.01	4.68e-06	3.00	1.034
	16384	4.15e-08	3.00	5.85e-07	3.00	1.034
	16	2.84e-05	—	6.66e-04	—	1.018
	64	1.79e-06	3.99	4.20e-05	3.99	1.021
3	256	1.12e-07	3.99	2.64e-06	3.99	1.022
	1024	7.04e-09	4.00	1.65e-07	4.00	1.022
	4096	4.40e-10	4.00	1.03e-08	4.00	1.023
	16384	2.76e-11	4.00	6.47e-10	4.00	1.023
k	N	e_h	order	η_h	order	eff
	16	1.18e-01	—	3.01e-01	—	0.759
	64	3.04e-02	1.96	1.01e-01	1.57	0.944
1	256	6.85e-03	2.15	4.82e-02	1.07	1.003
	1024	1.52e-03	2.17	1.52e-02	1.67	1.020
	4096	3.57e-04	2.09	3.83e-03	1.99	1.029
	16384	8.76e-05	2.03	9.61e-04	1.99	1.034
	16	7.70e-03	—	2.21e-02	—	0.913
	64	8.73e-04	3.14	4.90e-03	2.17	0.996
2	256	9.42e-05	3.21	1.22e-03	2.01	1.009
	1024	1.04e-05	3.17	1.92e-04	2.67	1.011
	4096	1.22e-06	3.10	2.41e-05	2.99	1.014
	16384	1.47e-07	3.05	3.03e-06	2.99	1.015
	16	2.25e-04	—	8.48e-04	—	0.971
	64	1.26e-05	4.16	1.05e-04	3.01	1.004
3	256	7.12e-07	4.14	1.33e-05	2.98	1.006
	1024	4.19e-08	4.09	1.05e-06	3.66	1.006
	4096	2.54e-09	4.05	6.64e-08	3.99	1.007
	16384	1.56e-10	4.02	4.17e-09	3.99	1.008
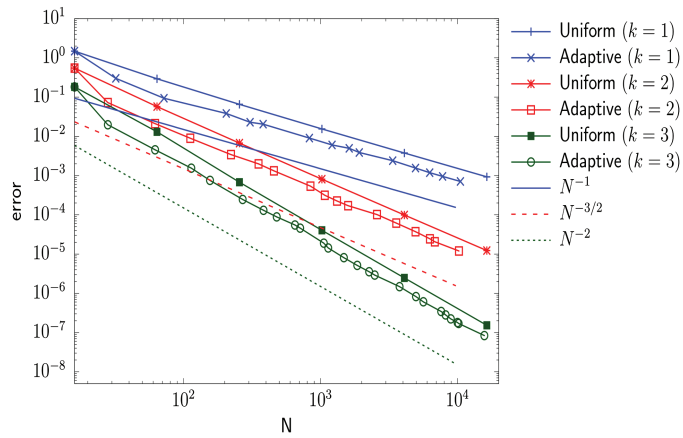
Fig. 1. History of convergence ($k = 1, 2, 3$) for $\mathbf{e}_h$ with uniform and adaptive ($\theta = 0.25$) refinements, for the Kovasznay flow.
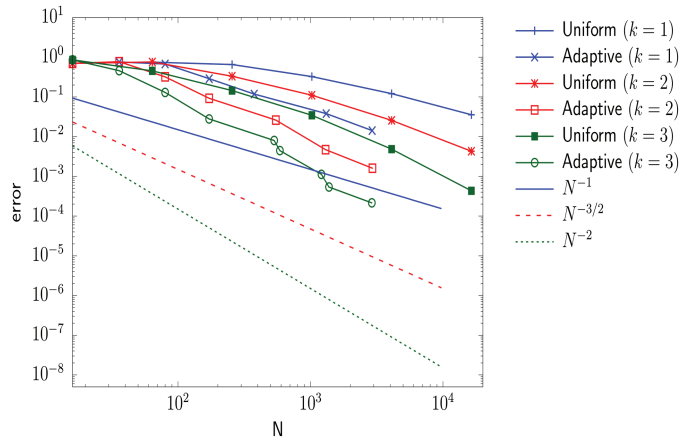

Fig. 2. History of convergence for $\mathbf{e}_h$ with uniform and adaptive ($\theta = 0.25$) refinement ($k = 1, 2, 3$), singularly perturbed problem.
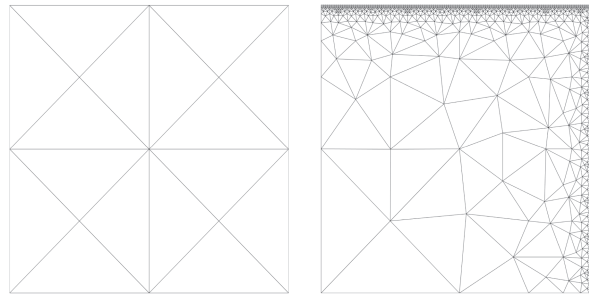

Fig. 3. Initial (left, 16 elements) and final adapted (right, 2920 elements) meshes for the singularly perturbed problem ($k = 1$).
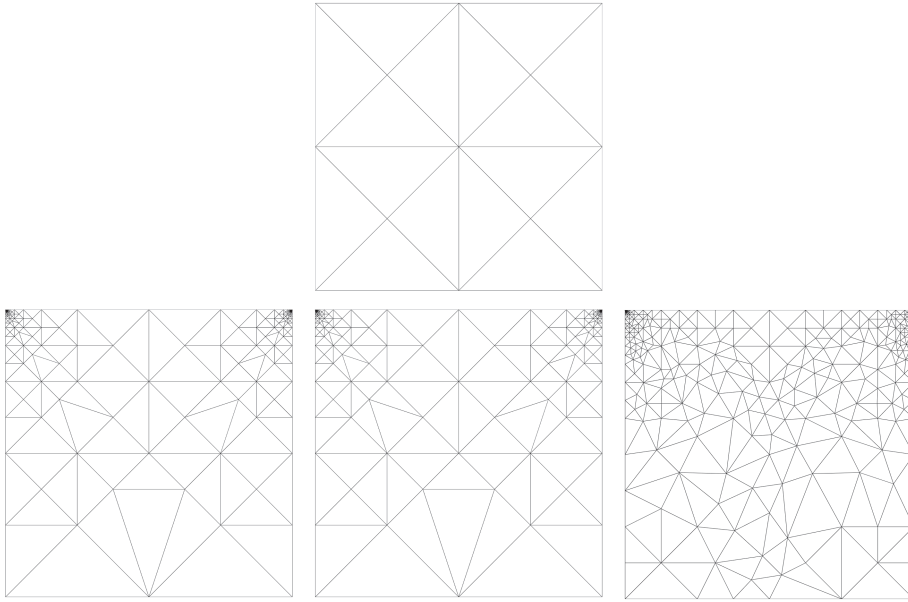
FIG. 4. Initial (top, 16 elements) and adapted (bottom) meshes for the cavity problem ($k = 1$) for $\tau = 10^{-2}$, 1 and 10^2 (left, center and right, respectively). Adapted meshes with 942 (first two) and 1200 elements (last one).

to the unresolved boundary layers. Figure 3 shows the initial mesh and the final mesh obtained with the adaptive scheme. We observe here how the estimator is properly localizing the boundary layers.

5.4 *The lid-driven cavity problem*

For this test, we use the same domain as in the previous experiment and $\tau = 10^{-2}, 1, 10^2$. We set $\nu = 1$, $\alpha = 0, f = 0$ and $u_D = (1, 0)$, on $x_2 = 1$, and 0 on the rest of the boundary of Ω. Note that two singularities arise at the top corners of the domain, due to the discontinuities on the boundary condition. This fact is captured by our estimator by refining mainly in those corners as can be seen in Fig. 4, where the initial and adapted ($\theta = 0.1$) meshes are displayed. We also note that the number of element of the adapted meshes does not change significantly even when we use different values of τ.

References

Ainsworth, M. (2007) A posteriori error estimation for discontinuous Galerkin finite element approximation. *SIAM J. Numer. Anal.*, **45**, 1777–1798.

Ainsworth, M. & Rankin, R. (2010) Fully computable error bounds for discontinuous Galerkin finite element approximations on meshes with an arbitrary number of levels of hanging nodes. *SIAM J. Numer. Anal.*, **47**, 4112–4141.

Becker, R., Hansbo, P. & Larson, M. G. (2003) Energy norm a posteriori error estimation for discontinuous Galerkin methods. *Comput. Methods Appl. Mech. Engrg.*, **192**, 723–733.

Braess, D., Fraunholz, T. & Hoppe, R. H. W. (2014) An equilibrated a posteriori error estimator for the interior penalty discontinuous Galerkin method. *SIAM J. Numer. Anal.*, **52**, 2121–2136.

Brinkman, H. C. (1947) A calculation of the viscous force exerted by a flowing fluid on a dense swarm of particles. *Appl. Sci. Res.*, **A 1**, 27–34.

Bustinza, R., Gatica, G. N. & Cockburn, B. (2005) An a posteriori error estimate for the local discontinuous Galerkin method applied to linear and nonlinear diffusion problems. *J. Sci. Comput.*, **22/23**, 147–185.

Carstensen, C., Gudi, T. & Jensen, M. (2009) A unifying theory of a posteriori error control for discontinuous Galerkin FEM. *Numer. Math.*, **112**, 363–379.

Castillo, P. (2005) An a posteriori error estimate for the local discontinuous Galerkin method. *J. Sci. Comput.*, **22/23**, 187–204.

Cesmelioglu, A., Cockburn, B. & Qiu, W. (2017) Analysis of a hybridizable discontinuous Galerkin method for the steady-state incompressible Navier–Stokes equations. *Math. Comput.*, **86**, 1643–1670.

Cesmelioglu, A., Cockburn, B., Nguyen, N. C. & Peraire, J. (2013) Analysis of HDG methods for Oseen equations. *J. Sci. Comput.*, **55**, 392–431.

Chen, H., Li, J. & Qiu, W. (2016) Robust a posteriori error estimates for HDG method for convection–diffusion equations. *IMA J. Numer. Anal.*, **36**, 437–462.

Clément, P. (1975) Approximation by finite element functions using local regularization. *Rev. Française Automat. Informat. Recherche Opérationnelle Sér.*, **9**, 77–84.

Cockburn, B. & Gopalakrishnan, J. (2009) The derivation of hybridizable discontinuous Galerkin methods for Stokes flow. *SIAM J. Numer. Anal.*, **47**, 1092–1125.

Cockburn, B. & Sayas, F.-J. (2014) Divergence-conforming HDG methods for Stokes flows. *Math. Comput.*, **83**, 1571–1598.

Cockburn, B. & Shu, C.-W. (1998) The local discontinuous galerkin method for time-dependent convection-diffusion systems. *SIAM J. Numer. Anal.*, **35**, 2440–2463.

Cockburn, B. & Zhang, W. (2012) A posteriori error estimates for HDG methods. *J. Sci. Comput.*, **51**, 582–607.

Cockburn, B. & Zhang, W. (2013) A posteriori error analysis for hybridizable discontinuous Galerkin methods for second order elliptic problems. *SIAM J. Numer. Anal.*, **51**, 676–693.

Cockburn, B. & Zhang, W. (2014) An a posteriori error estimate for the variable-degree Raviart-Thomas method. *Math. Comput.*, **83**, 1063–1082.

Cockburn, B., Dong, B. & Guzmán, J. (2008) A superconvergent LDG–hybridizable galerkin method for second-order elliptic problems. *Math. Comput.*, **77**, 1887–1916.

Cockburn, B., Guzmán, J. & Wang, H. (2009a) Superconvergent discontinuous Galerkin methods for second-order elliptic problems. *Math. Comput.*, **78**, 1–24.

Cockburn, B., Gopalakrishnan, J. & Lazarov, R. D. (2009b) Unified hybridization of discontinuous Galerkin, mixed, and continuous Galerkin methods for second order elliptic problems. *SIAM J. Numer. Anal.*, **47**, 1319–1365.

Cockburn, B., Gopalakrishnan, J. & Sayas, F.-J. (2010) A projection-based error analysis of HDG methods. *Math. Comput.*, **79**, 1351–1367.

Cockburn, B., Gopalakrishnan, J., Nguyen, N. C., Peraire, J. & Sayas, F.-J. (2011) Analysis of HDG methods for Stokes flow. *Math. Comput.*, **80**, 723–760.

COCHEZ-DHONDT, S. & NICAISE, S. (2008) Equilibrated error estimators for discontinuous Galerkin methods. *Numer. Methods Partial Differ. Equ.*, **24**, 1236–1252.

CREUSÉ, E. & NICAISE, S. (2010) A posteriori error estimator based on gradient recovery by averaging for discontinuous Galerkin methods. *J. Comput. Appl. Math.*, **234**, 2903–2915.

CREUSÉ, E. & NICAISE, S. (2013) A *posteriori* error estimator based on gradient recovery by averaging for convection-diffusion-reaction problems approximated by discontinuous Galerkin methods. *IMA J. Numer. Anal.*, **33**, 212–241.

DAUGE, M. (1989) Stationary Stokes and Navier–Stokes systems on two- or three-dimensional domains with corners. Part I. Linearized equations. *SIAM J. Math. Anal.*, **20**, 74–97.

DI PIETRO, D. A. & ERN, A. (2012) *Mathematical Aspects of Discontinuous Galerkin Methods.* Mathématiques & Applications, vol. 69. Berlin–Heilderber: Springer.

DOLEJŠÍ, V., ŠEBESTOVÁ, I. & VOHRALÍK, M. (2015) Algebraic and discretization error estimation by equilibrated fluxes for discontinuous Galerkin methods on nonmatching grids. *J. Sci. Comput.*, **64**, 1–34.

ERN, A. & VOHRALÍK, M. (2009) Flux reconstruction and a posteriori error estimation for discontinuous Galerkin methods on general nonmatching grids. *C. R. Math. Acad. Sci. Paris*, **347**, 441–444.

ERN, A. & VOHRALÍK, M. (2015) Polynomial-degree-robust a posteriori estimates in a unified setting for conforming, nonconforming, discontinuous Galerkin, and mixed discretizations. *SIAM J. Numer. Anal.*, **53**, 1058–1081.

ERN, A., NICAISE, S. & VOHRALÍK, M. (2007) An accurate H(div) flux reconstruction for discontinuous Galerkin approximations of elliptic problems. *C. R. Math. Acad. Sci. Paris*, **345**, 709–712.

ERN, A., STEPHANSEN, A. F. & VOHRALÍK, M. (2010) Guaranteed and robust discontinuous Galerkin a posteriori error estimates for convection-diffusion-reaction problems. *J. Comput. Appl. Math.*, **234**, 114–130.

FU, G., JIN, Y. & QIU, W. (2018) Parameter-free superconvergent H(div)-conforming HDG methods for the Brinkman equations. *IMA J. Numer. Anal.*, dry001.

FU, G., QIU, W. & ZHANG, W. (2015) An analysis of HDG methods for convection-dominated diffusion problems. *ESAIM: M2AN*, **49**, 225–256.

GATICA, G. N. & SEQUEIRA, F. A. (2015) Analysis of an augmented HDG method for a class of quasi-Newtonian Stokes flows. *J. Sci. Comput.*, **65**, 1270–1308.

GATICA, G. N. & SEQUEIRA, F. A. (2016) A priori and a posteriori error analyses of an augmented HDG method for a class of quasi-Newtonian Stokes flows. *J. Sci. Comput.*, **69**, 1192–1250.

GATICA, G. N. & SEQUEIRA, F. A. (2017) Analysis of the HDG method for the Stokes–Darcy coupling. *Numer. Methods Partial Differ. Equ.*, **33**, 885–917.

GATICA, L. F. & SEQUEIRA, F. A. (2018) A priori and a posteriori error analyses of an HDG method for the Brinkman problem. *Comput. Math. Appl.*, **75**, 1191–1212.

GIRAULT, V. & RAVIART, P.-A. (1986) *Finite Element Methods for Navier-Stokes Equations. Theory and Algorithms.* Springer Series in Computational Mathematics, vol. 5. Berlin: Springer.

GRIEBEL, M. & KLITZ, M. (2010) Homogenization and numerical simulation of flow in geometries with textile microstructures. *Multiscale Model. Simul.*, **8**, 1439–1460.

HOUSTON, P., SCHÖTZAU, D. & WIHLER, T. P. (2007) Energy norm a posteriori error estimation of *hp*-adaptive discontinuous Galerkin methods for elliptic problems. *Math. Models Methods Appl. Sci.*, **17**, 33–62.

KARAKASHIAN, O. A. & PASCAL, F. (2003) A posteriori error estimates for a discontinuous Galerkin approximation of second-order elliptic problems. *SIAM J. Numer. Anal.*, **41**, 2374–2399.

KARAKASHIAN, O. A. & PASCAL, F. (2007) Convergence of adaptive discontinuous Galerkin approximations of second-order elliptic problems. *SIAM J. Numer. Anal.*, **45**, 641–665.

KAYA, T. & GOLDAK, J. (2007) Three-dimensional numerical analysis of heat and mass transfer in heat pipes. *Heat Mass Transfer*, **43**, 775–785.

KELLOGG, R. B. & OSBORN, J. E. (1976) A regularity result for the Stokes problem in a convex polygon. *J. Funct. Anal.*, **21**, 397–431.

KOVASZNAY, L. I. G. (1948) Laminar flow behind a two-dimensional grid. *Proc. Camb. Philos. Soc.*, **44**, 58–62.

LAZAROV, R., REPIN, S. & TOMAR, S. K. (2009) Functional a posteriori error estimates for discontinuous Galerkin approximations of elliptic problems. *Numer. Methods Partial Differ. Equ.*, **25**, 952–971.

LI, X. (2005) *Principles of Fuel Cells*. New York: Taylor & Francis.

LOVADINA, C. & MARINI, L. D. (2009) A-posteriori error estimates for discontinuous Galerkin approximations of second order elliptic problems. *J. Sci. Comput.*, **40**, 340–359.

NGUYEN, N. C., PERAIRE, J. & COCKBURN, B. (2009a) An implicit high-order hybridizable discontinuous Galerkin method for linear convection–diffusion equations. *J. Comput. Phys.*, **228**, 3232–3254.

NGUYEN, N. C., PERAIRE, J. & COCKBURN, B. (2009b) An implicit high-order hybridizable discontinuous Galerkin method for nonlinear convection–diffusion equations. *J. Comput. Phys.*, **228**, 8841–8855.

NGUYEN, N. C., PERAIRE, J. & COCKBURN, B. (2010) A hybridizable discontinuous Galerkin method for Stokes flow. *Comput. Methods Appl. Mech. Eng.*, **199**, 582–597.

NGUYEN, N. C., PERAIRE, J. & COCKBURN, B. (2011) An implicit high-order hybridizable discontinuous Galerkin method for the incompressible Navier–Stokes equations. *J. Comput. Phys.*, **230**, 1147–1170.

PAYNE, L. E. & WEINBERGER, H. F. (1960) An optimal Poincaré inequality for convex domains. *Arch. Ration. Mech. Anal.*, **25**, 286–292.

RIVIÈRE, B. & WHEELER, M. F. (2003) A posteriori error estimates for a discontinuous Galerkin method applied to elliptic problems. Log number: R74. *Comput. Math. Appl.*, **46**, 141–163.

VERFÜRTH, R. (1998) A posteriori error estimators for convection–diffusion equations. *Numer. Math.*, **80**, 641–663.

VERFÜRTH, R. (2013) *A Posteriori Error Estimation Techniques for Finite Element Methods.* Numerical Mathematics and Scientific Computation. Oxford: Oxford University Press.

ZHU, L., GIANI, S., HOUSTON, P. & SCHÖTZAU, D. (2011) Energy norm a posteriori error estimation for hp-adaptive discontinuous Galerkin methods for elliptic problems in three dimensions. *Math. Models Methods Appl. Sci.*, **21**, 267–306.